Australian Government

Department of Defence

Defence Science and
Technology Group

Determination of Minimised K_t Values and Boundary Shapes for a Class of Quasi-Rectangular Holes in Infinite Plates

Witold Waldman

Aerospace Division
Defence Science and Technology Group

DST Group-TR-3125

ABSTRACT

Transferable solutions for stress-minimised quasi-rectangular holes in a two-dimensional infinite plate have been determined for a number of remote loading conditions and a wide range of hole aspect ratios. These include uniaxial, equibiaxial and reversed biaxial loading cases. The analytical shape and tangential stress equations for these quasi-rectangular holes can readily be used to obtain solutions for other specific biaxial loading cases that are of interest. The equation for the radius of curvature for these shapes has also been derived. Tables and plots of shape parameters and stress concentration factors are provided, enabling the stress-minimised quasi-rectangular hole shapes to be easily and rapidly applied by designers. These shapes produce peak stresses that are often within 10% of those obtained by free-form shape optimisation, and they can serve as initial shapes for subsequent free-form shape optimisation analyses. The source code for the program that was used to determine the stress-minimised quasi-rectangular hole shapes as a function of hole aspect ratio is provided, as is a set of functions that are suitable for use in spreadsheets. For the first time, these tools provide an automated procedure that enables a designer to set up a biaxial loading condition of interest and then determine sets of stress-minimised quasi-rectangular hole shapes that vary as a function of hole aspect ratio.

RELEASE LIMITATION

Approved for public release

Published by

Aerospace Division
Defence Science and Technology Group
506 Lorimer Street
Fishermans Bend, Victoria 3207, Australia

Telephone: 1300 333 362
Fax: (03) 9626 7999

AR-016-304
July 2015

APPROVED FOR PUBLIC RELEASE

Determination of Minimised K_t Values and Boundary Shapes for a Class of Quasi-Rectangular Holes in Infinite Plates

Executive Summary

Aerospace Division is extensively involved in developing technologies that reduce the cost of ownership of aircraft in service with the Royal Australian Air Force (RAAF) by extending the fatigue lives of airframe structural components. A shape optimisation technology, based on iterative finite element analysis techniques, has been developed and used by Aerospace Division to determine optimal repair profiles that can be applied to areas where stress concentrations have caused a location to become fatigue critical. Such optimal shapes produce significant reductions in peak stress as compared to typical non-optimal circular holes. However, iterative numerical analysis to determine optimal shapes is very computationally intensive and time consuming. A need therefore exists to have at hand sets of stress-minimised shapes that can be easily and rapidly used in repair applications.

Transferable solutions for stress-minimised quasi-rectangular holes in a two-dimensional infinite plate have been determined for a number of remote loading conditions and a wide range of hole aspect ratios. These include uniaxial, equibiaxial and reversed biaxial loading cases. The analytical shape and tangential stress equations for these quasi-rectangular holes can readily be used to obtain solutions for other specific biaxial loading cases that are of interest. The equation for the radius of curvature for these shapes has also been derived. Tables and plots of shape parameters and stress concentration factors are provided, enabling the stress-minimised quasi-rectangular hole shapes to be easily and rapidly applied by designers. These shapes produce peak stresses that are often within 10% of those obtained by free-form shape optimisation, and they can serve as initial shapes for subsequent free-form shape optimisation analyses. The source code for the program that was used to determine the stress-minimised quasi-rectangular hole shapes as a function of hole aspect ratio is provided, as is a set of functions that are suitable for use in spreadsheets. For the first time, these tools provide an automated procedure that enables a designer to set up a biaxial loading condition of interest and then determine sets of stress-minimised quasi-rectangular hole shapes that vary as a function of hole aspect ratio.

The families of quasi-rectangular hole shapes that have been developed in this report provide additional valuable insights into stress-minimised rework hole shapes. They also facilitate an improved capability for rapidly designing such rework shapes for use in RAAF structural repairs while significantly reducing the amplitudes of peak stresses that can lead to early fatigue failures. The parametric shape studies that were conducted here have increased the knowledge about the effectiveness of various hole shapes to significantly enhance the fatigue lives of RAAF airframe structural components. Structural engineers who are working on implementing lightening holes to create lightweight, structurally-efficient designs can also easily apply these shapes to improve the performance characteristics of their structures.

Author

Witold Waldman
Aerospace Division

Mr Witold Waldman completed a BEng (with distinction) in Aeronautical Engineering at the Royal Melbourne Institute of Technology in 1981. He commenced work in Structures Division in 1982 at what was then the Aeronautical Research Laboratory. He has published a number of papers and reports, and his experience has focussed on stress analysis using finite element and boundary element methods, structural mechanics, fracture mechanics, computational unsteady aerodynamics, structural dynamics testing, digital filtering of flight test data, nonlinear optimisation, and spectral analysis. His recent work has been in the areas of structural shape optimisation and computation of stress intensity factors. He is currently a Senior Research Engineer in the Structural and Damage Mechanics Group in the Airframe Technology and Safety Branch of Aerospace Division at Defence Science and Technology Group, Department of Defence.

Contents

Nomenclature

a	length of semimajor axis of ellipse
b	length of semiminor axis of ellipse
K_t	stress concentration factor
K_{tmax}	maximum stress concentration factor
K_{tmin}	minimum stress concentration factor
l	length of hole in plate
r	corner radius of square-like hole in plate
w	width of hole in plate
W	width of plate
x	rectangular Cartesian x-coordinate of hole boundary
$\dot{x}$	first derivative with respect to θ of x-coordinate of hole boundary
$\ddot{x}$	second derivative with respect to θ of x-coordinate of hole boundary
y	rectangular Cartesian y-coordinate of hole boundary
$\dot{y}$	first derivative with respect to θ of y-coordinate of hole boundary
$\ddot{y}$	second derivative with respect to θ of y-coordinate of hole boundary
α	shape parameter associated with quasi-rectangular hole
β	load axis misalignment angle
ε	shape parameter associated with quasi-rectangular hole
θ	parametric polar angle
λ	aspect ratio of hole, = l/w
ξ	angle of applied remote tension stress at infinity
ρ	radius of curvature
ρ_{min}	minimum radius of curvature
ρ_{max}	maximum radius of curvature
σ	applied remote tension stress at infinity
σ_x	applied remote direct stress in the x-direction
σ_y	applied remote direct stress in the y-direction
σ_θ	tangential stress around boundary of hole
$\sigma_{x'}$	transformed applied remote direct stress
$\sigma_{y'}$	transformed applied remote direct stress
$\tau_{x'y'}$	transformed applied remote shear stress
ψ	geometric polar angle of a point on hole boundary

1. Introduction

Holes are a common feature in aircraft and other engineering structures, and they are often prone to fatigue damage because of the stress concentrations that they introduce. Considerable prior work has been undertaken by Aerospace Division of Defence Science and Technology Group (DST Group) to determine precise optimal rework shapes to minimise the peak stresses occurring at existing holes and other stress concentrations in ageing aircraft structures, leading to substantial increases in fatigue life. The shapes were computed using finite element analysis (FEA) in conjunction with a custom-written FORTRAN program that implemented a fully-automated iterative gradientless shape optimisation algorithm (Heller *et al.* 1999), which has subsequently been significantly enhanced over many years (Waldman *et al.* 2001, Heller *et al.* 2002, Burchill and Heller 2004a, Burchill and Heller 2004b, McDonald and Heller 2004). It now includes features such as radius-of-curvature geometric constraints (Waldman *et al.* 2002), as well as the ability to simultaneously minimise multiple stress peaks (Waldman and Heller 2006, Waldman and Heller 2015).

The shapes that result from application of the DST Group gradientless shape optimisation method are fully free form in nature and do not rely on analytical functions to represent the boundary shape. However, they are generally computationally expensive to determine and, as a result, it is somewhat difficult and time consuming to perform parametric studies to obtain a better understanding of the parameters that are of importance for particular loading conditions. The shape optimisation process for holes also requires an initial "kick-off" shape, which is usually based on simple circular or elliptical hole shapes, or whatever hole geometry is originally present in the structural component under consideration. For some problems of interest, it is desirable to be able to define an initial hole shape that already bears some resemblance to an optimal hole, preferably based on analytical equations, as this can lead to more rapid convergence to the optimal solution, as well as smoother boundaries when the optimal shape is determined.

The topic of stress-minimising optimal holes in plates has been of considerable research interest for many decades. Even so, extremely few general analytical solutions exist, and those that do are only for some very specific loading cases. Durelli and Murray (1943) determined that an elliptical hole of aspect ratio *length*:*width* = l:w in a biaxial stress field of σ_x:σ_y = l:w (where $\sigma_x \geq \sigma_y$) produces a uniform distribution of tangential stress around the hole boundary equal to $(l/w+1)\sigma_x$ (as long as the two combined stresses are of the same sign). Under these conditions, the value of the uniform stress is much less than the maximum peak stress produced by a circular hole for the same loading, $(3l/w-1)\sigma_x$, unless σ_x:σ_y = 1:1, in which case the values are equal.

Some experimental and numerical analysis work has been carried on square-like holes to determine minimised values of stress concentration factor. Brock (1958) presented an exact analytical solution for the stresses around square holes with rounded corners of arbitrary corner radius, r, for the case of simple uniform uniaxial loading and a range of corner radius to hole width ratios, r/w. A minimum stress concentration factor of about 2.8 (7% lower than for a circular hole) was obtained for $r/w \approx 3/8$. A small number of experimentally-determined quasi-square hole shapes for a range of loadings were reported by Durelli and Rajaiah (1979, 1980, 1981), which had been obtained using photoelastic analysis techniques.

For the finite-width plates that were tested, the best reported hole shape produced a stress concentration factor of 2.54 for a hole width to plate width ratio of w/W = 0.14. Using the inverse of a finite-width correction for holes in plates obtained from Pilkey (2008), this stress concentration factor is reduced to 2.49 for the equivalent infinite plate case. Dhir (1981) developed an analytical/numerical procedure that enabled a class of square-like hole geometries to be studied for uniaxially-loaded or biaxially-loaded infinite plates, but yet again little transferable hole shape data was provided. For the case of uniaxial loading, Dhir (1981) obtained a minimum stress concentration factor of 2.47, which is about 1% lower than that which was obtained by Durelli and Rajaiah (1981).

Vigdergauz and Cherkayev (1986) studied single holes in an elastic plate loaded at infinity by mutually perpendicular tensile and compressive stresses ($\sigma_x\sigma_y < 0$), for which they determined values of stress concentration factors using a numerical method. They proposed a condition of optimality that the absolute magnitude of the tangential stress be constant almost everywhere around the boundary of the hole. They determined that the optimal hole shapes are almost rectangular, having curved sides with corners of a definite included angle, with the ratio of the sides and the included angles being dependent on the applied loading. As the stress fields near the corners were considerably distorted, they determined the stress concentration factors only for segments of the boundary lying near the middle of the sides. They did not present shape coefficients for their optimal hole shapes, except for one comparison with an existing solution, nor were any distributions of tangential stress provided.

Rajaiah and Naik (1983) have studied hole shapes with minimum stress concentration in infinite isotropic plates under in-plane loading conditions. They utilised well-known conformal transformation techniques to determine a set of closed-form analytical equations used for calculating the distribution of tangential stress around the boundary of quasi-rectangular holes (see Figure 1). These holes could be subjected to tension and/or compression loadings aligned with the major or minor axes of the hole, thus enabling many different uniaxial and biaxial loading scenarios to be easily investigated. Their solutions do not have any sharp corners, unlike those described by Vigdergauz and Cherkayev (1986), and thus are quite amenable to being manufactured. As a result of the rounded corners, they are also expected to be relatively robust if small variations from the assumed loading conditions occur.

The expressions derived by Rajaiah and Naik (1983) are compact in nature, as well as being exact for the geometry that is under consideration. The hole shapes are specified through the use of two independent parameters, and the stress-minimised shapes offer worthwhile reductions in stress concentration compared to traditional circular and elliptical shapes. Their analytical formulation is therefore highly suitable for use in obtaining data on families of easily-computed transferable hole shapes that provide minimised values of stress concentration.

Section 2 describes the analytical equations that can be used for computing hole shapes and their associated distributions of tangential stress. In a new development, closed-form equations for the radius of curvature are also given. In order to validate the equations, Section 3 presents some comparisons with the results obtained from other known solutions.

In Section 4, the method used to compute the families of shapes is outlined, and sets of results obtained for a wide range of typical uniaxial and biaxial loading cases that are of engineering interest are provided. These include the shape parameters and the associated K_t values. Finally, the conclusion is given in Section 5.

2. Analytical equations for a class of quasi-rectangular holes in 2D plates

As mentioned previously, Rajaiah and Naik (1983) have derived a set of equations for computing the tangential stress distribution around the boundary of quasi-rectangular holes in infinite two-dimensional plates under general biaxial in-plane remote loading conditions. Their formulation will be used here to conduct a series of parametric studies to determine the variation in stress concentration factor, K_t, for quasi-rectangular holes of different aspect ratios under a variety of uniaxial and biaxial loading conditions.

2.1 Equations for shape of hole boundary

Consider a general quasi-rectangular hole in a biaxially-loaded infinite plate, where the idealised geometry is as shown in Figure 1. The boundary contour of the hole is given by the following two equations:

$$x = a\,(\cos\theta + \varepsilon\cos 3\theta) \tag{1}$$

$$y = a\,(\alpha\sin\theta - \varepsilon\sin 3\theta) \tag{2}$$

where θ is the polar angle that changes from 0° to 360° when going around the boundary of the hole, α and ε are hole shape parameters that can take on values in the range $0 < \alpha \le 1$ and $-0.12 \le \varepsilon \le 0$, and a is the semimajor axis of the hole. For general values of α and ε, the opening is elongated in the x-direction. When $\alpha = 1$ and $\varepsilon = 0$, a circular hole of radius a is obtained. An elliptical hole shape results when the value of $\varepsilon = 0$ and $\alpha < 1$ (and in this instance the aspect ratio of the elliptical holes is $1/\alpha$).

2.2 Equations for tangential stress around hole boundary

When the plate is subjected to a remote tension stress σ_x aligned with the x-axis (see Figure 1), which is the major axis of the opening, Rajaiah and Naik (1983) have determined that the tangential stress around the hole boundary due to this load, $\sigma_{\theta x}$, is given by the equation:

$$\begin{aligned}\sigma_{\theta x} = \Big\{&\left(B^2/C^2\right) + \left(1/C^2\right)\{\alpha(-A\cos\theta + 2B\sin\theta) \\ &- \varepsilon\left[4A\alpha\cos\theta/(1+\alpha) - 3A\cos 3\theta + 2B\left(-2\alpha\sin\theta/(1+\alpha) + 3\sin 3\theta\right)\right] \\ &- 8\varepsilon^2\alpha(A\cos\theta - B\sin\theta)/(1+\alpha)^2\}\Big\}\sigma_x\end{aligned} \tag{3}$$

Similarly, when the plate is subjected to a remote tension stress σ_y aligned with the y-axis (see Figure 1), which is the minor axis of the opening, the tangential stress around the hole boundary due to this load, $\sigma_{\theta y}$, is given by the following equation:

$$\sigma_{\theta y} = \Big\{\left(A^2/C^2\right) + \left(1/C^2\right)\{2A\cos\theta - B\sin\theta + \varepsilon\left[2A\left(2\cos\theta/(1+\alpha) + 3\cos 3\theta\right) - 4B\sin\theta/(1+\alpha) - 3B\sin 3\theta\right] + 8\varepsilon^2(A\cos\theta - B\sin\theta)/(1+\alpha)^2\}\Big\}\sigma_y \quad (4)$$

where

$$A = \alpha\cos\theta - 3\varepsilon\cos 3\theta$$
$$B = \sin\theta + 3\varepsilon\sin 3\theta$$
$$C^2 = A^2 + B^2$$

The total tangential stress around the hole boundary, σ_θ, due to the independent action of the remote stresses σ_x and σ_y, is therefore given by the following equation:

$$\sigma_\theta = \sigma_{\theta x} + \sigma_{\theta y} \quad (5)$$

2.3 Equation for radius of curvature around hole boundary

In order to assist in the assessment of the machinability of quasi-rectangular hole shapes, it is useful to be able to compute the radius of curvature around the boundary of such holes. The radius of curvature ρ corresponding to the boundary shape defined by the expressions in Equations (1) and (2) can be easily computed using the following equation:

$$\rho(\theta) = \left|\frac{(\dot{x}^2+\dot{y}^2)^{3/2}}{\dot{x}\ddot{y} - \dot{y}\ddot{x}}\right| \quad (6)$$

where

$$\dot{x} = a\,(-\sin\theta - 3\varepsilon\sin 3\theta)$$
$$\ddot{x} = a\,(-\cos\theta - 9\varepsilon\cos 3\theta)$$
$$\dot{y} = a\,(\alpha\cos\theta - 3\varepsilon\cos 3\theta)$$
$$\ddot{y} = a\,(-\alpha\sin\theta + 9\varepsilon\sin 3\theta)$$

For an ellipse with a major axis of length $l = 2a$ and a minor axis of width of $w = 2b$, the minimum and maximum radii of curvature, ρ_{min} and ρ_{max}, are:

$$\rho_{min} = b^2/a \quad \text{at the vertices of the major axis} \quad (7)$$
$$\rho_{max} = a^2/b \quad \text{at the vertices of the minor axis} \quad (8)$$

For an ellipse, we also have that $\alpha = b/a$. Hence, the normalised minimum and maximum radii of curvature are given by the following two expressions:

$$\rho_{min}/w = \alpha/2 \quad (9)$$
$$\rho_{max}/w = 1/(2\alpha^2) \quad (10)$$

3. Comparison with other solutions

The previously described formulas for the boundary shape of the quasi-rectangular hole and the tangential stress σ_θ, from which K_t values may be readily calculated, have been implemented in a Microsoft Excel spreadsheet using the Visual Basic for Applications (VBA) programming language. The source code listing of the various functions is provided in Appendix A, and the spreadsheet can be requested from the author if desired. In the three following subsections, the K_t results computed by using these formulas have been compared to some other known solutions for particular cases, as well as against results obtained by an alternative general-purpose numerical analysis technique.

3.1 Original results from Rajaiah and Naik (1983)

As an initial check on the correctness of the programming of the equations for the quasi-rectangular hole, K_t results were computed for the various loading and geometry cases that had previously been analysed by Rajaiah and Naik (1983). Table 1 shows the results obtained from the present work, as well as those originally published by Rajaiah and Naik. It is seen that the results from the present implementation are in excellent agreement with those of Rajaiah and Naik for all of the cases that they originally considered.

3.2 Tangential stress around circular holes

The formula for the distribution of tangential stress σ_θ around a circular hole due to a biaxial stress field consisting of remote stresses σ_x and σ_y is well known, and is given here as

$$\sigma_\theta = \left[1 - 2\cos 2\theta\right]\sigma_x + \left[1 - 2\cos 2(\theta - \pi/2)\right]\sigma_y \tag{11}$$

By substituting $\alpha = 1$ and $\varepsilon = 0$ into Equations (3) and (4), after a little algebraic manipulation it can be shown that we obtain Equation (11).

Figure 2 shows the results obtained for the K_t distribution around one-quarter of the boundary of a circular hole in a plate with a biaxial loading $\sigma_x{:}\sigma_y = 1{:}{-1}$, using the equations for the circular hole and the quasi-rectangular hole with shape parameters $\varepsilon = 0$ and $\alpha = 1$. This demonstrates the expected exact agreement between the two sets of results.

3.3 Tangential stress around elliptical holes

Consider the stretching of an infinite plate containing an elliptical hole that is free from external stresses. The stress state at infinity is a tension stress whose magnitude is σ in a direction forming an angle ξ with the x-axis. Muskhelishvili (1953) has obtained the following compact expression for the tangential stress σ_θ around the boundary of the ellipse

$$\sigma_\theta = \frac{1 - m^2 + 2m\cos 2\xi - 2\cos 2(\theta - \xi)}{1 - 2m\cos 2\theta + m^2}\,\sigma \tag{12}$$

where

$$m = \frac{a-b}{a+b} = \frac{l-w}{l+w} = \frac{l/w - 1}{l/w + 1} \tag{13}$$

and a is the length of the semimajor axis of the ellipse aligned in the x-direction, b is the length of semiminor axis of the ellipse aligned in the y-direction, $l = 2a$ is the length of the ellipse, and $w = 2b$ is the width of the ellipse. Here the (x, y) coordinates defining the shape of the ellipse can be determined from the expressions $x = a\cos\theta$ and $y = b\sin\theta$. It is noted that if $m = 0$ (when $a = b$) then the shape becomes a circle. Alternative solutions to this problem have also been obtained by Inglis (1913), Durelli and Murray (1943), Brown (1977) and Gao (1996). The analytical solutions obtained by Brown (1977) and Gao (1996) also permit the calculation of the full-field elastic stresses and displacements around an elliptical hole.

For the case of a stress field consisting of the remote direct stresses σ_x and σ_y and a remote shear stress τ_{xy}, it is possible to obtain the solution for the tangential stress by summation. The contribution that is due to σ_x is obtained by substituting $\sigma = \sigma_x$ and $\xi = 0$ into Equation (12), while the contribution due to σ_y is obtained by substituting $\sigma = \sigma_y$ and $\xi = \pi/2$, and the contributions due to τ_{xy} are obtained by substituting $\sigma = \tau_{xy}$ and $\xi = \pi/4$ and also $\sigma = -\tau_{xy}$ and $\xi = 3\pi/4$. Performing the summation leads to the following expression for the total tangential stress around the boundary of the ellipse

$$\sigma_\theta = \frac{1+2m-m^2-2\cos 2\theta}{1-2m\cos 2\theta+m^2}\sigma_x + \frac{1-2m-m^2+2\cos 2\theta}{1-2m\cos 2\theta+m^2}\sigma_y - \frac{4\sin 2\theta}{1-2m\cos 2\theta+m^2}\tau_{xy} \qquad (14)$$

For elliptical holes, there are some relatively simple test cases that can be conveniently analysed. Under tensile biaxial loading conditions σ_x:σ_y ($\tau_{xy} = 0$), the optimal stress-minimising ellipse has a corresponding aspect ratio of l:$w = \sigma_x$:σ_y, and the stress concentration factor is constant around the entire boundary of the ellipse and is given by $K_t = (1+l/w)$. When these combinations of loading and ellipse geometry were utilised, the results obtained when using Equations (3) and (4) were in complete agreement with those obtained when using Equation (14).

Figure 3 shows the tangential stress distribution for an elliptical hole with aspect ratio l:w = 5:2 and biaxial loading σ_x:σ_y = –2:1 ($\tau_{xy} = 0$), and compares the results that were computed using Equations (3) and (4) with those obtained using Equation (14). The two sets of results are in complete agreement.

3.4 Tangential stress around quasi-rectangular holes

Although the Sections 3.3 and 3.3 were helpful in establishing the correctness of the equations used for characterising the shape and tangential stress distribution for quasi-rectangular holes, they were somewhat limited in their scope because they utilised $\varepsilon = 0$ exclusively. It is therefore desirable to check the accuracy of the equations using a test case where $\varepsilon \neq 0$. This can be done by setting up and analysing a finite element model of the chosen geometry and loading. This would require approximating the infinite plate solution by utilising a very large plate in order to minimise finite-width effects on the solution.

A boundary element analysis code that was originally developed by Chang and Mear (1995) has the ability to deal with infinite domains as part of its formulation. This code has been provided to DST Group by Newman *et al*. (2006) in a computer program called FADD2D that runs under the 32-bit edition of Microsoft Windows XP. The FADD2D code was used to

perform an independent analysis of a test case involving a quasi-rectangular hole with geometry parameters $\varepsilon = -0.0876$ and $\alpha = 0.5269$ for a remote biaxial loading of $\sigma_x:\sigma_y = 1: -1$.

In order to do this, Equations (1) and (2) were used to compute a series of points along the boundary of the quasi-rectangular hole. These points were then used to create a FADD2D input deck (see Appendix A) in which the hole geometry was specified using a total of 36 parabolic segments. Each of these parabolic segments was defined using three sequential points, and each segment was itself subdivided into two boundary elements. The shape of the quasi-rectangular hole that was studied is shown in Figure 4a.

A comparison between the two sets of K_t distributions around one-quarter of the hole boundary is shown in Figure 4b. It is evident that there is excellent agreement between the results produced by the FADD2D boundary element analysis code and the equations developed by Rajaiah and Naik (1983). The FADD2D code computed values of $K_{tmax} = 2.846$ and $K_{tmin} = -3.712$, while the equations produced $K_{tmax} = 2.849$ and $K_{tmin} = -3.718$. In both cases the differences here are less than 0.2%.

If desired, it is also possible to check the robustness of the quasi-rectangular hole designs to small amounts of loading misalignment. This can be achieved in the FADD2D code by specifying appropriate combinations of remote direct stress and shear stress in order to simulate the desired angular amount of loading misalignment, while keeping the orientation of the hole geometry constant. Consider again a system of remote direct stresses defined by σ_x and σ_y (see Figure 1). If we wish to rotate the original applied loading by an angle β in the clockwise direction, then the new equivalent remote loading consisting of the transformed direct stresses $\sigma_{x'}$ and $\sigma_{y'}$ and shear stress $\tau_{x'y'}$ can be determined by using the expressions

$$\sigma_{x'} = \sigma_x \cos^2\beta + \sigma_y \sin^2\beta \quad (15)$$

$$\sigma_{y'} = \sigma_x \sin^2\beta + \sigma_y \cos^2\beta \quad (16)$$

$$\tau_{x'y'} = (\sigma_y - \sigma_x) \sin\beta \cos\beta \quad (17)$$

3.5 Free-form gradientless shape optimisation solutions

A number of solutions for holes are available that were obtained using the DST Group free-form shape optimisation method that utilises iterative finite element analysis (Burchill and Heller 2004b, Waldman and Heller 2006, Waldman and Heller 2015). The equivalent load cases and geometries were analysed using the quasi-rectangular hole formulation proposed by Rajaiah and Naik (1983) in order to determine the stress concentration factors, and the results are presented in Table 2. It is evident that stress-minimised quasi-rectangular hole solutions can often produce peak K_t values that are quite close in value to those obtained through FEA-based free-form shape optimisation, often to within 10% or less.

In general, the K_t values determined using quasi-rectangular holes are somewhat greater in magnitude. This is to be expected, as the geometric form of a quasi-rectangular hole is constrained by its shape equations, whereas the FEA-based shape optimisation method has no such restrictions because it is free-form in nature, other than possible user-applied minimum radius of curvature constraints.

Looking at the results in Table 2 for the uniaxial loading case (σ_x:σ_y = 1:0), as the shape of the holes becomes more elongated in the direction of the applied load, it is evident that the stress-minimised quasi-rectangular holes produce K_t values that get progressively closer to those from the free-form FEA solutions. When $\lambda = 1$, the quasi-rectangular hole has a K_t that is 13.3% higher, but by $\lambda = 5$ the difference has reduced to 1.8%. Even by $\lambda = 2$, the difference is only 8.1%. This trend in the quasi-rectangular hole results is also evident in the other loading cases that are presented in Table 2.

Figure 5 shows the shapes and K_t distributions for two square-like hole designs obtained for the uniaxial remote loading of σ_x:σ_y = 0:1 and hole aspect ratios of $\lambda \approx 1$. One of the holes was determined using the method of Rajaiah and Naik (1983). Its aspect ratio is $\lambda = 1$, and the computed shape parameters are $\varepsilon = -0.0545$ and $\alpha = 1$, and it has peak K_t values of 2.469 and –0.911 and $\rho_{min}/w = 0.248$. The other hole was determined using the free-form FEA-based multiple stress peak shape optimisation method of Waldman and Heller (2015). Its aspect ratio is $\lambda = 0.9803$ (it is slightly higher than it is wide), and it has peak K_t values of 2.259 and –0.836 and $\rho_{min}/w = 0.143$ (a geometric restriction that was set for this selected shape optimisation case).

Looking at Figure 5a, it is clear that the two shapes are quite different. The shape obtained using the method of Rajaiah and Naik (1983) is much more circular and entirely concave, and has a larger minimum radius of curvature as a result of the geometric restrictions imposed on it by Equations (1) and (2). On the other hand, the FEA-obtained optimal shape has much tighter corner radii, and is convex in shape at the top and bottom where the stresses are compressive. Looking at Figure 5b, it is noted that the optimal shape obtained using FEA-based shape optimisation has much longer and more uniform regions of K_t, in both the tensile and compressive regions. Nonetheless, the two shapes both offer a significant reduction of the peak tensile K_t value versus that produced by a standard circular hole.

4. Computation of the minimum K_t and the hole shape

Using Equations (1) to (4), a FORTRAN program was written to numerically determine the values of α and ε for stress-minimised quasi-rectangular holes under general biaxial remote loading conditions of σ_x:σ_y (see Appendix C). A set of holes with aspect ratios $\lambda = l/w$ varying over the range $\lambda = 1, 1.25, 1.5, \ldots 4$ were studied. We note that the value of the parameter α of each such hole is approximately equal to the reciprocal of the aspect ratio, $\alpha \approx 1/\lambda$. By utilising this feature, it is therefore possible to set up a search of the α and ε parameter space, involving computing the boundary coordinates (and hence the true aspect ratio of the hole, λ) and the minimum and maximum K_t values, K_{tmin} and K_{tmax}, for each associated shape. Quarter-symmetry conditions were taken advantage of in order to help minimise the computational load, and values of $\theta = 0°, 0.125°, 0.250°, \ldots 90°$ were used to produce a fine angular resolution of 0.125° when determining the peak K_t values. The shape parameter ε was varied incrementally and covered the range of values $\varepsilon = 0, -0.0001, -0.002, \ldots -0.1200$. Similarly, the shape parameter α was varied incrementally, covering the range $0.90/\lambda \le \alpha \le 1.10/\lambda$ in steps of 0.0001. In the event that the value of the upper limit exceeded 1, the range $0.80/\lambda \le \alpha \le 1/\lambda$ was used instead. From the computed results, it was then possible to determine the values of α and ε that produce a minimum value of $\text{Max}(|K_{tmin}|, |K_{tmax}|)$ for each desired hole aspect ratio λ.

4.1 Computed values of α and ε for remote loading of σ_x:σ_y = 1:0

Table 3 presents the computed K_t values for stress-minimised quasi-rectangular hole shapes and standard elliptical hole shapes in an infinite plate under a uniaxial remote loading of σ_x:σ_y = 1:0 for the selected range of aspect ratios λ. The values of the two shape parameters ε and α for each optimal solution are also given, allowing the user to easily compute the hole shape using Equations (1)–(2), as well as the distribution of tangential stress σ_θ around the hole boundary using Equations (3)–(5). For the dual purposes of completeness and ease of comparison with the optimal values, the α values for the equivalent elliptical shapes have also been provided.

Figure 6a plots the variation in K_t with increasing hole aspect ratio for the stress-minimised quasi-rectangular and the elliptical hole shapes in an infinite plate under a uniaxial remote loading of σ_x:σ_y = 1:0. For this loading condition, the K_t decreases with increasing aspect ratio λ. Figure 6b shows the corresponding behaviour of the shape parameters α and ε for the stress-minimised quasi-rectangular holes. These curves can be used to determine with good accuracy the K_t values and shape parameters of stress-minimised quasi-rectangular holes for hole aspect ratios in the range $1 \le \lambda \le 4$. Figure 6a also shows two results obtained using the gradientless multi-peak shape optimisation method of Waldman and Heller (2006), and it is evident that the quasi-rectangular shapes have produced higher K_t values.

Figure 7 shows the shapes and K_t distributions for two stress-minimised quasi-rectangular holes for the uniaxial remote loading of σ_x:σ_y = 1:0 and hole aspect ratios of λ = 1 and 2. The shape with aspect ratio λ = 2 produces a zone where the stress is quite uniform in the region $55° \le \theta \le 90°$. For the case of a hole geometry with an aspect ratio of λ = 1, the quasi-square hole with rounded corners (ε = –0.0544 and α = 0.9996) offers a useful stress reduction of 17.7% compared to the circular hole. This hole shape also produces a zone where the stress is relatively uniform in the region $60° \le \theta \le 90°$, although there is a clearly defined peak in K_t that occurs at θ = 66.5° which is 5.0% greater than the value at θ = 90°.

4.2 Computed values of α and ε for remote loading of σ_x:σ_y = 0:1

In a similar manner, Table 4 presents the computed K_t values for stress-minimised quasi-rectangular hole shapes and standard elliptical hole shapes in an infinite plate under a uniaxial remote loading of σ_x:σ_y = 0:1, together with the values of the two shape parameters ε and α for each optimal solution. This loading is in a direction perpendicular to the major axis of the hole. Figure 8a plots the variation in K_t with increasing hole aspect ratio λ for both the stress-minimised quasi-rectangular holes and the elliptical holes. For this loading condition, the K_t increases with increasing aspect ratio. Figure 8b shows the corresponding behaviour of the shape parameters α and ε for the stress-minimised quasi-rectangular holes.

Figure 9 shows the shapes and K_t distributions for two stress-minimised quasi-rectangular holes for the uniaxial remote loading of σ_x:σ_y = 0:1 and hole aspect ratios of λ = 1 and 2. The shape with aspect ratio λ = 2 produces a zone of relatively uniform positive stress in the region $0° \le \theta \le 32°$.

4.3 Computed values of α and ε for remote loading of σ_x:σ_y = 1:1

Table 5 presents the computed K_t values for stress-minimised quasi-rectangular hole shapes and standard elliptical hole shapes in an infinite plate under a biaxial remote loading of σ_x:σ_y = 1:1, together with the values of the two shape parameters ε and α for each optimal solution. Figure 10a plots the variation in K_t with increasing hole aspect ratio λ for both the stress-minimised quasi-rectangular holes and the elliptical holes. For this loading condition, the K_t increases with increasing aspect ratio. Figure 10b shows the corresponding behaviour of the shape parameters α and ε for the stress-minimised quasi-rectangular holes.

Figure 11 shows the shapes and K_t distributions for two stress-minimised quasi-rectangular holes for the biaxial remote loading of σ_x:σ_y = 1:1 and hole aspect ratios of λ = 1 and 2. The shape with aspect ratio λ = 1 produces a zone where the stress is completely uniform over the entire hole boundary, which corresponds to the region 0° ≤ θ ≤ 90° in the plot. In comparison, the zone of nominally uniform stress for the hole with aspect ratio λ = 2 is considerably shorter, extending over the region 0° ≤ θ ≤ 32° in the plot.

4.4 Computed values of α and ε for remote loading of σ_x:σ_y = 1:–1

Table 6 presents the computed K_t values for stress-minimised quasi-rectangular hole shapes and standard elliptical hole shapes in an infinite plate under a reversed biaxial remote loading of σ_x:σ_y = 1:–1, together with the values of the two shape parameters ε and α for each optimal solution. Figure 12a plots the variation in K_t with increasing hole aspect ratio λ for both the stress-minimised quasi-rectangular holes and the elliptical holes. For this loading condition, the K_t increases with increasing aspect ratio λ. Figure 12b shows the corresponding behaviour of the shape parameters α and ε for the stress-minimised quasi-rectangular holes.

It is noted that the curve for the ε shape parameter in Figure 12b has a distinctly undulating nature, a feature that is absent from the results for the other loading conditions. The reason for this is not entirely understood, but it could be something to do with a relative insensitivity of the K_t values to small changes in ε, as in this instance the ε parameter covers a relatively small range of values, –0.0906 < ε < –0.0850. For example, using the computational results provided in Table 4, consider the data point (K_{tmax}, K_{tmin}, λ, α, ε) = (2.9481, –3.2548, 1.250, 0.8184, –0.0906). If we change the value of ε from –0.0906 to –0.0894, so that it lies midway between the adjacent two points on the curve, we obtain (K_{tmax}, K_{tmin}, λ, α, ε) = (2.9432, –3.2547, 1.249, 0.8184, –0.0894). This small but noticeable change in ε has produced a negligible change in K_{tmin} of around 0.003%, with a very small (0.08%) change in the value of the aspect ratio λ. On that basis, these two results can be regarded as being essentially the same, even though the relative change in ε was about 1.3%. Hence, it appears that the undulations in the ε curve can be neglected for our purposes.

Figure 13 shows the shapes and K_t distributions for two stress-minimised quasi-rectangular holes for the reversed biaxial remote loading of σ_x:σ_y = 1:–1 and hole aspect ratios of λ = 1 and 2. The shape with aspect ratio λ = 1 produces a zone where the tensile portion of the tangential stress distribution is relatively uniform over a small section of the hole boundary, corresponding to the region 60° ≤ θ ≤ 90° in the plot.

4.5 Computed values of α and ε for remote loading of σ_x:σ_y = –1:1

Table 7 presents the computed K_t values for stress-minimised quasi-rectangular hole shapes and standard elliptical hole shapes in an infinite plate under a reversed biaxial remote loading of σ_x:σ_y = –1:1, together with the values of the two shape parameters ε and α for each optimal solution. Figure 14a plots the variation in K_t with increasing hole aspect ratio λ for both the stress-minimised quasi-rectangular holes and the elliptical holes. For this loading condition, the K_t increases with increasing aspect ratio λ. Figure 14b shows the corresponding behaviour of the shape parameters α and ε for the stress-minimised quasi-rectangular holes. Figure 14a also shows the result obtained using the DST Group gradientless multi-peak free-form FEA shape optimisation method of Waldman and Heller (2006) for λ = 1, and it is evident that the quasi-rectangular shape has produced a slightly higher K_t value.

Figure 15 shows the shapes and K_t distributions for two stress-minimised quasi-rectangular holes for the biaxial remote loading of σ_x:σ_y = –1:1 and hole aspect ratios of λ = 1 and 2. The hole shape with aspect ratio λ = 1 produces a zone where the tensile portion of the tangential stress distribution is relatively uniform over a small section of the hole boundary, corresponding to the region 0° ≤ θ ≤ 30° in the plot. For this case, the quasi-square hole with rounded corners (ε = –0. 0.0896 and α = 1) offers a useful stress reduction of 23.2% compared to the circular hole.

4.6 Computed values of α and ε for remote loading of σ_x:σ_y = 2:1

Table 8 presents the computed K_t values for stress-minimised quasi-rectangular holes shapes and standard elliptical hole shapes in an infinite plate under a biaxial remote loading of σ_x:σ_y = 2:1, together with the values of the two shape parameters ε and α for each optimal solution. Figure 16a plots the variation in K_t with increasing hole aspect ratio λ for both the stress-minimised quasi-rectangular holes and the elliptical holes. For this loading condition, the K_t value first decreases with increasing hole aspect ratio until an aspect ratio of λ = 2.0 is reached, which corresponds to the well-known optimal condition of minimum K_t. As the aspect ratio continues to increase, the K_t value then increases as well. Figure 16b shows the corresponding behaviour of the shape parameters α and ε for the stress-minimised quasi-rectangular holes. It is noted that when the K_t is at its minimum value then ε = 0, and the optimal hole shape is that of an l:w = 2:1 ellipse.

Figure 17 shows the shapes and K_t distributions for two stress-minimised quasi-rectangular holes for the biaxial remote loading of σ_x:σ_y = 2:1 and hole aspect ratios of λ = 1 and 3. For the hole geometry with aspect ratio λ = 1, the quasi-square hole with rounded corners (ε = –0.0287 and α = 0.9996) offers a useful reduction in peak stress of 11.3% compared to the peak stress produced by the circular hole. The shape with aspect ratio λ = 3 produces a zone where the tensile portion of the tangential stress distribution is relatively uniform over a small section of the hole boundary, corresponding to the region 0° ≤ θ ≤ 30° in the plot. For this particular loading, Durelli and Murray (1943) have shown that the optimal solution is an ellipse with an aspect ratio of λ = 2 (also see Figure 16), which produces a constant K_t = 3 around the entire boundary of the ellipse. From the plots of the K_t distributions in Figure 17b,

it is evident that the lines showing the variation in the K_t values straddle a line of constant K_t = 3, with their maxima and minima falling either side of K_t = 3.

5. Conclusion

Using the formulation developed by Rajaiah and Naik (1983), extensive sets of transferable solutions for a single stress-minimised quasi-rectangular hole in an infinite plate have now been determined. These were obtained for a number of commonly-analysed biaxial remote loading conditions and a wide range of hole aspect ratios, $1 \leq \lambda \leq 4$. The equation for the radius of curvature around the hole boundary was also derived in this study. As the equations for the quasi-rectangular holes are applicable to general biaxial remote loadings, they can be readily used to obtain solutions for specific loading cases that may also be of interest. The quasi-rectangular hole formulation as implemented here was in excellent agreement with other known analytical solutions for circular and elliptical holes, as well as solutions obtained using other numerical techniques, so it can be used with confidence.

Comprehensive tables and plots of the hole shape parameters, α and ε, as well as the resulting K_t values, have been provided. These enable the quasi-rectangular hole shapes to be easily used by designers, with particular applicability to lightening holes used in the creation of lightweight, structurally-efficient designs. These stress-minimised shapes can also serve as initial shapes for subsequent free-form shape optimisation analyses, using methods such as the DST Group iterative FEA-based shape optimisation method, to obtain more accurate optimal solutions minimising the peak stresses around the hole boundary. For hole aspect ratios close to $\lambda = 1$, the quasi-rectangular shapes determined here produce peak stresses that are often within 10–15% of those obtained by free-form shape optimisation. For holes having larger aspect ratios, this improves to 5% or so.

To aid in the transferability of the work and results that have been presented in this report, the source code for a set of functions written in Visual Basic for Applications and suitable for use in Excel spreadsheets is listed in an Appendix. The source code for the FORTRAN 90 program used to determine the stress-minimised quasi-rectangular hole shapes as a function of aspect ratio is also provided in another Appendix. This program can be used to determine stress-minimised quasi-rectangular shapes for additional specific loading cases not studied here.

6. Acknowledgement

The author would like to thank Professor Mark E Mear, University of Texas at Austin, and Professor James C Newman Jr, Mississippi State University, for providing access to the FADD2D boundary element analysis code that was utilised in this report.

7. References

Brock JS, 1958: The stresses around square holes with rounded corners. *Journal of Ship Research*, October, pp 37–41.

Brown DK, 1977: A computer program to calculate the elastic stress and displacement fields around an elliptical hole under any applied plane state of stress. Computers & Structures, Vol 7, pp 571–580.

Burchill M, Heller M, 2004a: Optimal notch shapes for loaded plates. *Journal of Strain Analysis for Engineering Design*, Vol 39, No 1, pp 99–116.

Burchill M, Heller M, 2004b: Optimal free-form shapes for holes in flat plates under uniaxial and biaxial loading. *Journal of Strain Analysis for Engineering Design*, Vol 39, No 6, pp 595–614.

Chang C, Mear ME, 1995: A boundary element method for two dimensional linear elastic fracture analysis. *International Journal of Fracture*, Vol 74, pp 219–251.

Dhir SK, 1981: Optimization of a class of hole shapes in plate structures. *Journal of Applied Mechanics*, Vol 48, December, pp 905–908.

Durelli AJ, Murray WM, 1943: Stress distribution around an elliptical discontinuity in any two-dimensional, uniform and axial, system of combined stress. *Proceedings of the Society for Experimental Stress Analysis*, Vol 1, No 1, pp 19–31.

Durelli AJ, Rajaiah K, 1979: Optimum hole shapes in finite plates under uniaxial load. *Journal of Applied Mechanics*, Vol 46, September, pp 691–695.

Durelli AJ, Rajaiah K, 1980: Lighter and stronger. *Experimental Mechanics*, Vol 20, No 11, November, pp 369–380.

Durelli AJ, Rajaiah K, 1981: Quasi-square hole with optimum shape in an infinite plate subjected to in-plane loading. *Transactions of the ASME, Journal of Mechanical Design*, Vol 103, October, pp 866–870.

Gao X-L, 1996: A general solution of an infinite elastic plate with an elliptic hole under biaxial loading. International Journal of Pressure Vessels and Piping, Vol 67, pp 95–104.

Heller M, Kaye R, Rose LRF, 1999: A gradientless procedure for shape optimisation. *Journal of Strain Analysis for Engineering Design*, Vol 34, No 5, pp 323–336.

Heller M, McDonald M, Burchill M, Watters KC, 2002: F-111 airframe life extension through rework shape optimisation of critical features in the wing pivot fitting. In: Proceedings of the 6th Joint FAA/DoD/NASA Aging Aircraft Conference, 16–19 September, San Francisco, USA.

Heller M, Burchill M, Wescott R, Waldman W, Kaye R, Evans R, McDonald M, 2009: Airframe life extension by optimised shape reworking – overview of DSTO developments. In: 'ICAF 2009, Bridging the Gap between Theory and Operational Practice', Proceedings of the 25th Symposium of the International Committee on Aeronautical Fatigue, MJ Bos (Ed), 27–29 May, Rotterdam, The Netherlands.

Inglis CE, 1913: Stresses in a plate due to the presence of cracks and sharp corners. *Transactions of the Institute of Naval Architects*, Vol 55, pp 219–241.

McDonald M, Heller M, 2004: Robust shape optimization of notches for fatigue-life extension. *Structural and Multidisciplinary Optimization*, Vol 28, No 1, pp 55–68.

Muskhelishvili NI, 1953: *Some basic problems of the mathematical theory of elasticity*. Third Edition, P Noordhoff Ltd, Groningen, Holland.

Newman Jr JC, Chang C, Xiao L, Mear ME, Kale VJ, 2006: FADD2D: Fracture Analysis by Distributed Dislocations, Version 1.0, User Guide for Personal Computers with Demonstration Example, October.

Pilkey WD, Pilkey DF, 2008: *Peterson's Stress Concentration Factors*. Third Edition, John Wiley & Sons, Inc., ISBN: 978-0-470-04824-5.

Rajaiah K, Naik NK, 1983: Hole shapes with minimum stress concentration in infinite isotropic plates using conformal transformation. *ISME Journal of Engineering Design*, Vol 1, No 1, April, pp 15–19.

Vigdergauz SB, Cherkayev AV, 1986: A hole in plate, optimal for its biaxial extension-compression. *Journal of Applied Mathematics and Mechanics*, Vol 50, No 3, pp 401–404 (*Prikl. Matem. Mekhan.*, Vol 50, No 3, pp 524–528, 1986).

Waldman W, Heller M, Chen G, 2001: Optimal free-form fillet shapes for tension and bending. *International Journal of Fatigue*, Vol 23, pp 509–523.

Waldman W, Heller M, McDonald M, Chen G, 2002: Developments in rework shape optimisation for life extension of aging airframes. In: 'Applied Mechanics: Progress and Applications', Proceedings of the 3rd Australasian Congress on Applied Mechanics, edited by L Zhang, L Tong, J Gal, 20–22 February, Sydney, Australia, pp 695–702.

Waldman W, Heller M, 2006: Shape optimisation of holes for multi-peak stress minimisation. *Australian Journal of Mechanical Engineering*, Vol 3, No 1, pp 61–71.

Waldman W, Heller M, 2015: Shape optimisation of holes in loaded plates by minimisation of multiple stress peaks. Defence Science and Technology Organisation Research Report DSTO-RR-0412, Aerospace Division, Department of Defence, Melbourne, Australia.

Table 1: *K_t values for quasi-rectangular holes in an infinite plate subject to various uniaxial and biaxial remote loading conditions. Comparison of present work with the original results from Rajaiah and Naik (1983).*

Loading Case σ_x:σ_y	α	ε	K_t		
			Present Work	Rajaiah & Naik (1983)	Elliptical Hole ($\varepsilon = 0$)
1:1[1]	1.000	0.0	2.0000	2.00	2.0000
1:0	1.000	–0.055	2.4689	2.47	3.0000
1:–1	1.000	–0.09	3.0739	3.06	4.0000
1:0	0.537	–0.02	1.9017	1.90	2.0740
0:1	0.537	–0.07	3.2435	3.23	4.7244
1:1	0.537	–0.03	2.9774	2.97	3.7244
1:–1	0.537	–0.10	–3.7184	–3.69	–5.7244

[1] Exact stress-minimised optimal shape is a circular hole with $K_t = 2$.

Table 2: *Minimised K_t values for quasi-rectangular holes in an infinite plate subject to various uniaxial and biaxial remote loading conditions. Comparison of present work with that of DST Group free-form gradientless FEA shape optimisation method.*

Loading Case σ_x:σ_y	Aspect Ratio λ	Present Work				Elliptical Hole ($\varepsilon = 0$)	DST Group FEA Method		Present Work c.f. DST Group FEA Method
		α	ε	K_t	ρ_{min}/w	K_t	K_t	ρ_{min}/w	Difference
1:0	1	0.9996	–0.0544	2.468	0.249	3.000	2.178	0.075	+13.3%
1:0	2	0.5098	–0.0198	1.862	0.387	2.000	1.722	0.075	+8.1%
1:0	3	0.3401	–0.0102	1.607	0.229	1.667	1.534	0.075	+4.8%
1:0	4	0.2547	–0.0063	1.467	0.160	1.500	1.427	0.075	+2.8%
1:0	5	0.2032	–0.0040	1.380	0.121	1.400	1.356	0.075	+1.8%
1:–1	1	1.0000	–0.0898	3.074	0.163	4.000	2.912	0.100	+5.6%
1.377:–1	1	0.9996	–0.0822	2.895	0.178	3.726	2.707	0.050	+6.9%
1.377:–1	1.329	0.7701	–0.0713	2.686	0.157	5.035	2.525	0.050	+6.4%
1.377:–1	2	0.5232	–0.0933	3.947	0.154	6.377	3.020	0.111	+30.7%
2:1	1	0.9996	–0.0287	4.437	0.342	5.000	3.993	0.000	+11.1%
2:1[1]	2	0.5000	0.0000	3.000	0.250	3.000	2.991	0.000	+0.3%
3:1	1	0.9996	–0.0377	6.894	0.305	8.000	6.096	0.000	+13.1%
3:1	2	0.5034	–0.0070	4.858	0.293	5.000	4.644	0.000	+4.6%
3:1[2]	3	0.3333	0.0000	4.000	0.167	4.000	4.000	0.000	0.0%
4:1	1	0.9996	–0.0420	9.357	0.289	11.000	8.295	0.075	+12.8%
4:1	2	0.5098	–0.0198	6.718	0.321	7.000	6.360	0.075	+5.6%

[1] Exact stress-minimised optimal shape is an elliptical hole of aspect ratio $\lambda = 2$ with $K_t = 3$.

[2] Exact stress-minimised optimal shape is an elliptical hole of aspect ratio $\lambda = 3$ with $K_t = 4$.

Table 3: *Shape parameters ε and α and K_t values for stress-minimised quasi-rectangular holes and elliptical hole shapes of various aspect ratios in an infinite plate under a uniaxial remote loading of σ_x:σ_y = 1:0.*

Aspect Ratio	σ_x:σ_y = 1:0								
	Stress-Minimised Shapes					Elliptical Holes (ε = 0)			
λ	ε	α	K_{tmax}	K_{tmin}	ρ_{min}/w	α	K_{tmax}	K_{tmin}	ρ_{min}/w
1.000	–0.0544	0.9996	2.4684	–0.9117	0.2489	1.0000	3.0000	–1.0000	0.5000
1.250	–0.0400	0.8077	2.2500	–0.9264	0.3120	0.8000	2.6000	–1.0000	0.4000
1.500	–0.0307	0.6767	2.0874	–0.9379	0.3631	0.6667	2.3333	–1.0000	0.3333
1.750	–0.0241	0.5816	1.9616	–0.9474	0.3926	0.5714	2.1429	–1.0000	0.2857
2.000	–0.0198	0.5098	1.8615	–0.9543	0.3870	0.5000	2.0000	–1.0000	0.2500
2.250	–0.0161	0.4533	1.7800	–0.9608	0.3365	0.4444	1.8889	–1.0000	0.2222
2.500	–0.0136	0.4081	1.7124	–0.9656	0.2910	0.4000	1.8000	–1.0000	0.2000
2.750	–0.0118	0.3711	1.6555	–0.9691	0.2573	0.3636	1.7273	–1.0000	0.1818
3.000	–0.0102	0.3401	1.6068	–0.9725	0.2293	0.3333	1.6667	–1.0000	0.1667
3.250	–0.0086	0.3136	1.5648	–0.9761	0.2047	0.3077	1.6154	–1.0000	0.1538
3.500	–0.0077	0.2912	1.5282	–0.9782	0.1872	0.2857	1.5714	–1.0000	0.1429
3.750	–0.0069	0.2717	1.4959	–0.9801	0.1721	0.2667	1.5333	–1.0000	0.1333
4.000	–0.0063	0.2547	1.4674	–0.9815	0.1597	0.2500	1.5000	–1.0000	0.1250

Table 4: *Shape parameters ε and α and K_t values for stress-minimised quasi-rectangular holes and elliptical hole shapes of various aspect ratios in an infinite plate under a uniaxial remote loading of σ_x:σ_y = 0:1.*

Aspect Ratio	σ_x:σ_y = 0:1								
	Stress-Minimised Shapes					Elliptical Holes (ε = 0)			
λ	ε	α	K_{tmax}	K_{tmin}	ρ_{min}/w	α	K_{tmax}	K_{tmin}	ρ_{min}/w
1.000	–0.0544	1.0000	2.4688	–0.9116	0.2486	1.0000	3.0000	–1.0000	0.5000
1.250	–0.0590	0.8121	2.7054	–0.8966	0.2434	0.8000	3.5000	–1.0000	0.4000
1.500	–0.0619	0.6875	2.9099	–0.8853	0.2411	0.6667	4.0000	–1.0000	0.3333
1.750	–0.0647	0.5993	3.0882	–0.8755	0.2384	0.5714	4.5000	–1.0000	0.2857
2.000	–0.0656	0.5318	3.2482	–0.8693	0.2414	0.5000	5.0000	–1.0000	0.2500
2.250	–0.0663	0.4767	3.3992	–0.8678	0.2441	0.4444	5.5000	–1.0000	0.2222
2.500	–0.0666	0.4308	3.5425	–0.8706	0.2476	0.4000	6.0000	–1.0000	0.2000
2.750	–0.0673	0.3916	3.6795	–0.8763	0.2488	0.3636	6.5000	–1.0000	0.1818
3.000	–0.0679	0.3578	3.8108	–0.8841	0.2500	0.3333	7.0000	–1.0000	0.1667
3.250	–0.0679	0.3286	3.9372	–0.8928	0.2534	0.3077	7.5000	–1.0000	0.1538
3.500	–0.0683	0.3026	4.0591	–0.9030	0.2548	0.2857	8.0000	–1.0000	0.1429
3.750	–0.0681	0.2799	4.1778	–0.9128	0.2589	0.2667	8.5000	–1.0000	0.1333
4.000	–0.0692	0.2584	4.2916	–0.9263	0.2563	0.2500	9.0000	–1.0000	0.1250

Table 5: *Shape parameters ε and α and K_t values for stress-minimised quasi-rectangular holes and elliptical hole shapes of various aspect ratios in an infinite plate under an equibiaxial remote loading of σ_x:σ_y = 1:1.*

Aspect Ratio	σ_x:σ_y = 1:1								
	Stress-Minimised Shapes					Elliptical Holes (ε = 0)			
λ	ε	α	K_{tmax}	K_{tmin}	ρ_{min}/w	α	K_{tmax}	K_{tmin}	ρ_{min}/w
1.000	0.0000	1.0000	2.0000	2.0000	0.5000	1.0000	2.0000	2.0000	0.5000
1.250	–0.0120	0.8027	2.3244	1.4851	0.4403	0.8000	2.5000	1.6000	0.4000
1.500	–0.0208	0.6738	2.6006	1.1659	0.4044	0.6667	3.0000	1.3333	0.3333
1.750	–0.0271	0.5832	2.8385	0.9538	0.3832	0.5714	3.5000	1.1429	0.2857
2.000	–0.0320	0.5161	3.0456	0.8023	0.3699	0.5000	4.0000	1.0000	0.2500
2.250	–0.0358	0.4644	3.2277	0.6897	0.3622	0.4444	4.5000	0.8889	0.2222
2.500	–0.0389	0.4234	3.3890	0.6027	0.3579	0.4000	5.0000	0.8000	0.2000
2.750	–0.0415	0.3901	3.5329	0.5333	0.3561	0.3636	5.5000	0.7273	0.1818
3.000	–0.0434	0.3619	3.6644	0.4774	0.3567	0.3333	6.0000	0.6667	0.1667
3.250	–0.0446	0.3366	3.7907	0.4306	0.3589	0.3077	6.5000	0.6154	0.1538
3.500	–0.0459	0.3139	3.9130	0.3881	0.3600	0.2857	7.0000	0.5714	0.1429
3.750	–0.0474	0.2933	4.0315	0.3486	0.3595	0.2667	7.5000	0.5333	0.1333
4.000	–0.0481	0.2747	4.1460	0.3164	0.3618	0.2500	8.0000	0.5000	0.1250

Table 6: *Shape parameters ε and α and K_t values for stress-minimised quasi-rectangular holes and elliptical hole shapes of various aspect ratios in an infinite plate under a reversed biaxial remote loading of σ_x:σ_y = 1:–1.*

Aspect Ratio	σ_x:σ_y = 1:–1								
	Stress-Minimised Shapes					Elliptical Holes (ε = 0)			
λ	ε	α	K_{tmax}	K_{tmin}	ρ_{min}/w	α	K_{tmax}	K_{tmin}	ρ_{min}/w
1.000	–0.0896	1.0000	3.0739	–3.0739	0.1626	1.0000	4.0000	–4.0000	0.5000
1.250	–0.0906	0.8184	2.9482	–3.2548	0.1611	0.8000	3.6000	–4.5000	0.4000
1.500	–0.0889	0.6938	2.8842	–3.4182	0.1657	0.6667	3.3333	–5.0000	0.3333
1.750	–0.0883	0.6002	2.8578	–3.5720	0.1677	0.5714	3.1429	–5.5000	0.2857
2.000	–0.0876	0.5269	2.8487	–3.7180	0.1700	0.5000	3.0000	–6.0000	0.2500
2.250	–0.0870	0.4677	2.8511	–3.8573	0.1721	0.4444	2.8889	–6.5000	0.2222
2.500	–0.0865	0.4187	2.8613	–3.9911	0.1739	0.4000	2.8000	–7.0000	0.2000
2.750	–0.0861	0.3773	2.8772	–4.1200	0.1756	0.3636	2.7273	–7.5000	0.1818
3.000	–0.0861	0.3415	2.9025	–4.2444	0.1759	0.3333	2.6667	–8.0000	0.1667
3.250	–0.0853	0.3113	2.9155	–4.3650	0.1793	0.3077	2.6154	–8.5000	0.1538
3.500	–0.0855	0.2837	2.9482	–4.4821	0.1788	0.2857	2.5714	–9.0000	0.1429
3.750	–0.0850	0.2601	2.9677	–4.5960	0.1813	0.2667	2.5333	–9.5000	0.1333
4.000	–0.0850	0.2384	2.9983	–4.7071	0.1817	0.2500	2.5000	–10.0000	0.1250

Table 7: *Shape parameters ε and α and K_t values for stress-minimised quasi-rectangular holes and elliptical hole shapes of various aspect ratios in an infinite plate under a reversed biaxial remote loading of σ_x:σ_y = –1:1.*

Aspect Ratio	σ_x:σ_y = –1:1								
	Stress-Minimised Shapes					Elliptical Holes (ε = 0)			
λ	ε	α	K_{tmax}	K_{tmin}	ρ_{min}/w	α	K_{tmax}	K_{tmin}	ρ_{min}/w
1.000	–0.0897	0.9996	3.0742	–3.0735	0.1624	1.0000	4.0000	–4.0000	0.5000
1.250	–0.0724	0.8142	3.3096	–2.9089	0.2045	0.8000	4.5000	–3.6000	0.4000
1.500	–0.0607	0.6867	3.6240	–2.7878	0.2451	0.6667	5.0000	–3.3333	0.3333
1.750	–0.0523	0.5937	3.9861	–2.6951	0.2826	0.5714	5.5000	–3.1429	0.2857
2.000	–0.0456	0.5227	4.3577	–2.6217	0.3173	0.5000	6.0000	–3.0000	0.2500
2.250	–0.0404	0.4668	4.7294	–2.5624	0.3457	0.4444	6.5000	–2.8889	0.2222
2.500	–0.0366	0.4219	5.0873	–2.5133	0.3653	0.4000	7.0000	–2.8000	0.2000
2.750	–0.0332	0.3847	5.4573	–2.4721	0.3772	0.3636	7.5000	–2.7273	0.1818
3.000	–0.0306	0.3537	5.8149	–2.4370	0.3788	0.3333	8.0000	–2.6667	0.1667
3.250	–0.0282	0.3272	6.1836	–2.4067	0.3686	0.3077	8.5000	–2.6154	0.1538
3.500	–0.0262	0.3044	6.5489	–2.3804	0.3450	0.2857	9.0000	–2.5714	0.1429
3.750	–0.0245	0.2846	6.9113	–2.3572	0.3162	0.2667	9.5000	–2.5333	0.1333
4.000	–0.0231	0.2673	7.2655	–2.3367	0.2929	0.2500	10.0000	–2.5000	0.1250

Table 8: *Shape parameters ε and α and K_t values for stress-minimised quasi-rectangular holes and elliptical hole shapes of various aspect ratios in an infinite plate under a biaxial remote loading of σ_x:σ_y = 2:1.*

Aspect Ratio	σ_x:σ_y = 2:1								
	Stress-Minimised Shapes					Elliptical Holes (ε = 0)			
λ	ε	α	K_{tmax}	K_{tmin}	ρ_{min}/w	α	K_{tmax}	K_{tmin}	ρ_{min}/w
1.000	–0.0287	0.9996	4.4374	0.7348	0.3417	1.0000	5.0000	1.0000	0.5000
1.250	–0.0160	0.8029	3.9227	1.2625	0.4230	0.8000	4.2000	1.5000	0.4000
1.500	–0.0085	0.6693	3.5373	1.8150	0.3955	0.6667	3.6667	2.0000	0.3333
1.750	–0.0033	0.5727	3.2381	2.4010	0.3072	0.5714	3.2857	2.5000	0.2857
2.000	0.0000	0.5000	3.0000	3.0000	0.2500	0.5000	3.0000	3.0000	0.2500
2.250	–0.0063	0.4480	3.2339	2.6863	0.2616	0.4444	3.5000	2.7778	0.2222
2.500	–0.0114	0.4069	3.4400	2.4472	0.2741	0.4000	4.0000	2.6000	0.2000
2.750	–0.0156	0.3736	3.6231	2.2595	0.2872	0.3636	4.5000	2.4546	0.1818
3.000	–0.0191	0.3461	3.7869	2.1087	0.3005	0.3333	5.0000	2.3333	0.1667
3.250	–0.0219	0.3229	3.9342	1.9867	0.3124	0.3077	5.5000	2.2308	0.1538
3.500	–0.0243	0.3031	4.0678	1.8846	0.3245	0.2857	6.0000	2.1429	0.1429
3.750	–0.0266	0.2862	4.1891	1.7960	0.3392	0.2667	6.5000	2.0667	0.1333
4.000	–0.0285	0.2714	4.3001	1.7211	0.3524	0.2500	7.0000	2.0000	0.1250

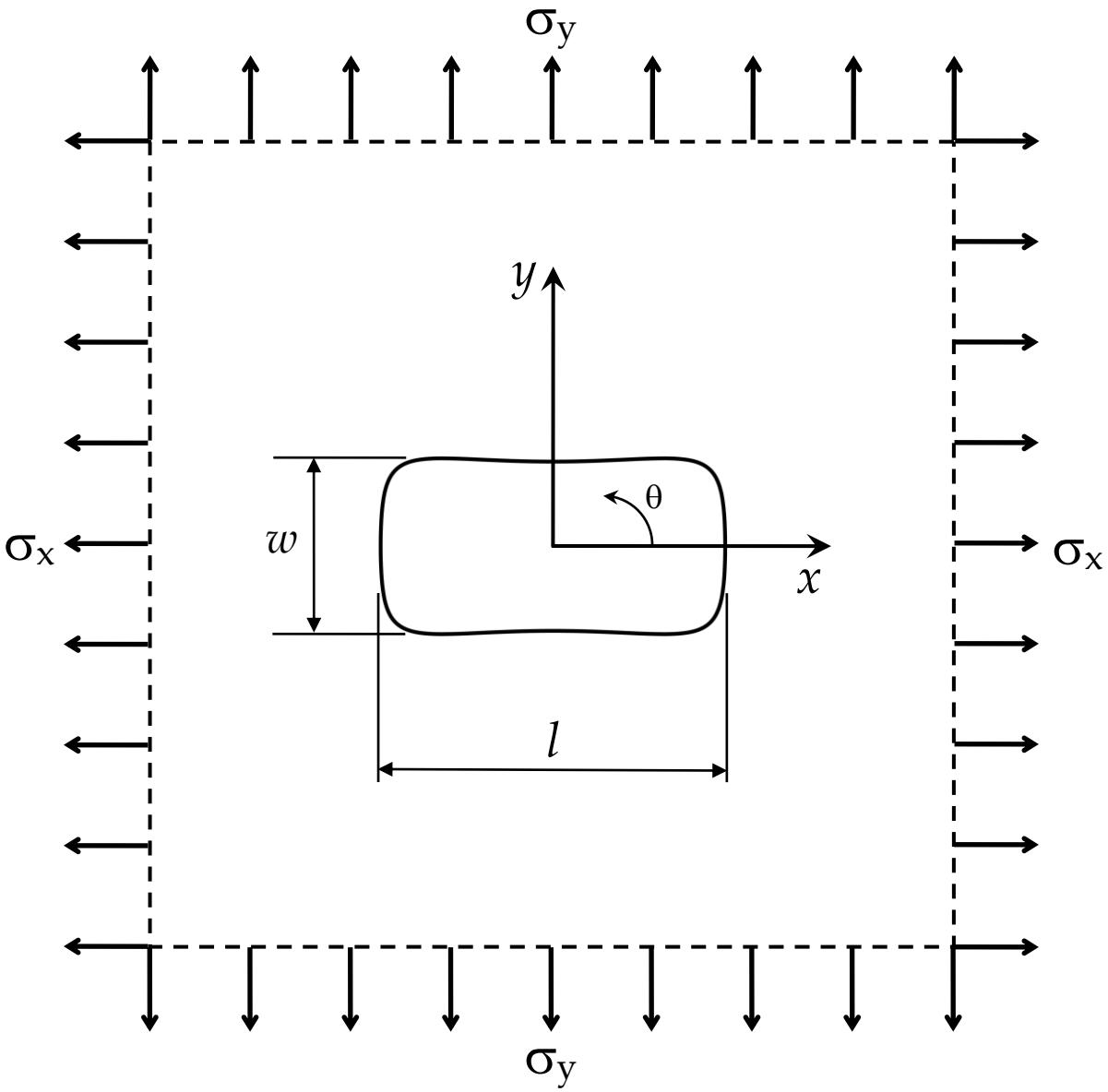

Figure 1: *Idealised geometry and loading for a quasi-rectangular hole of aspect ratio l:w in a biaxially-loaded infinite plate.*

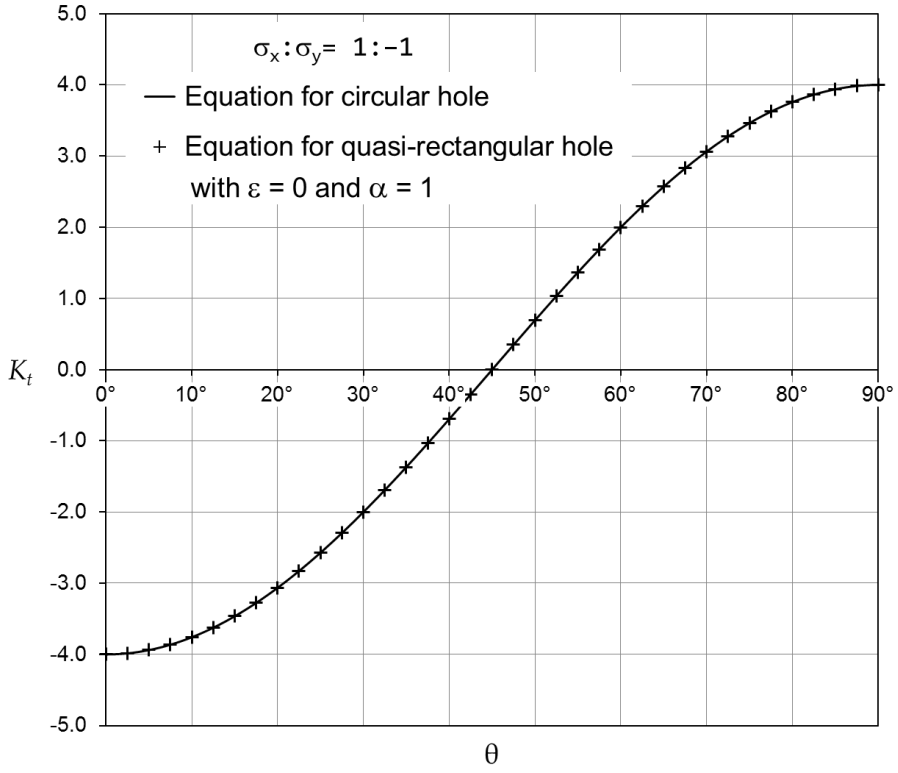

Figure 2: *K_t distribution around one-quarter of boundary of a circular hole in a plate under remote biaxial loading σ_x:σ_y = 1:–1, using the equations for a circular hole and the quasi-rectangular hole with shape parameters $\varepsilon = 0$ and $\alpha = 1$.*

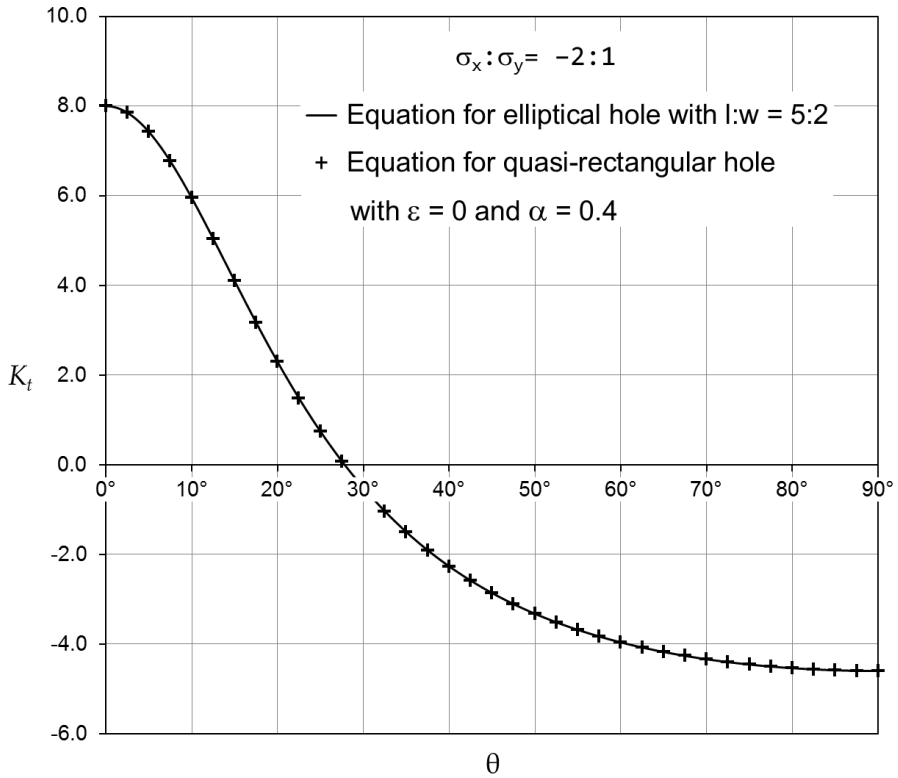

Figure 3: *K_t distribution around one-quarter of boundary of an elliptical hole of aspect ratio l:w = 5:2 in a plate under remote biaxial loading σ_x:σ_y = –2:1, using the equations for an elliptical hole and the quasi-rectangular hole with shape parameters $\varepsilon = 0$ and $\alpha = 0.4$.*

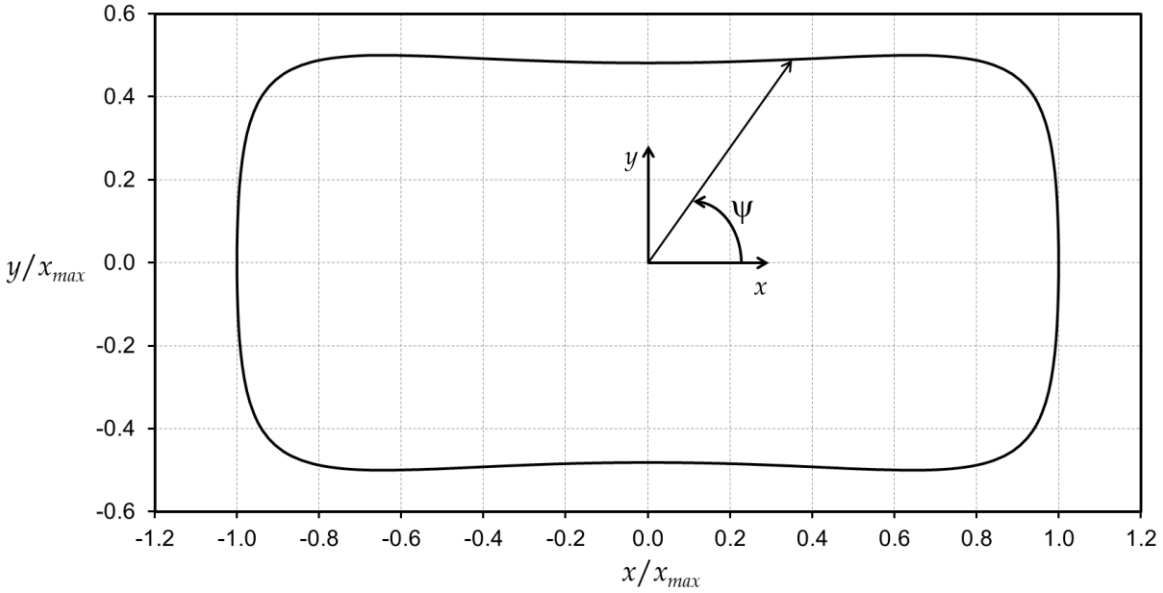

(a)

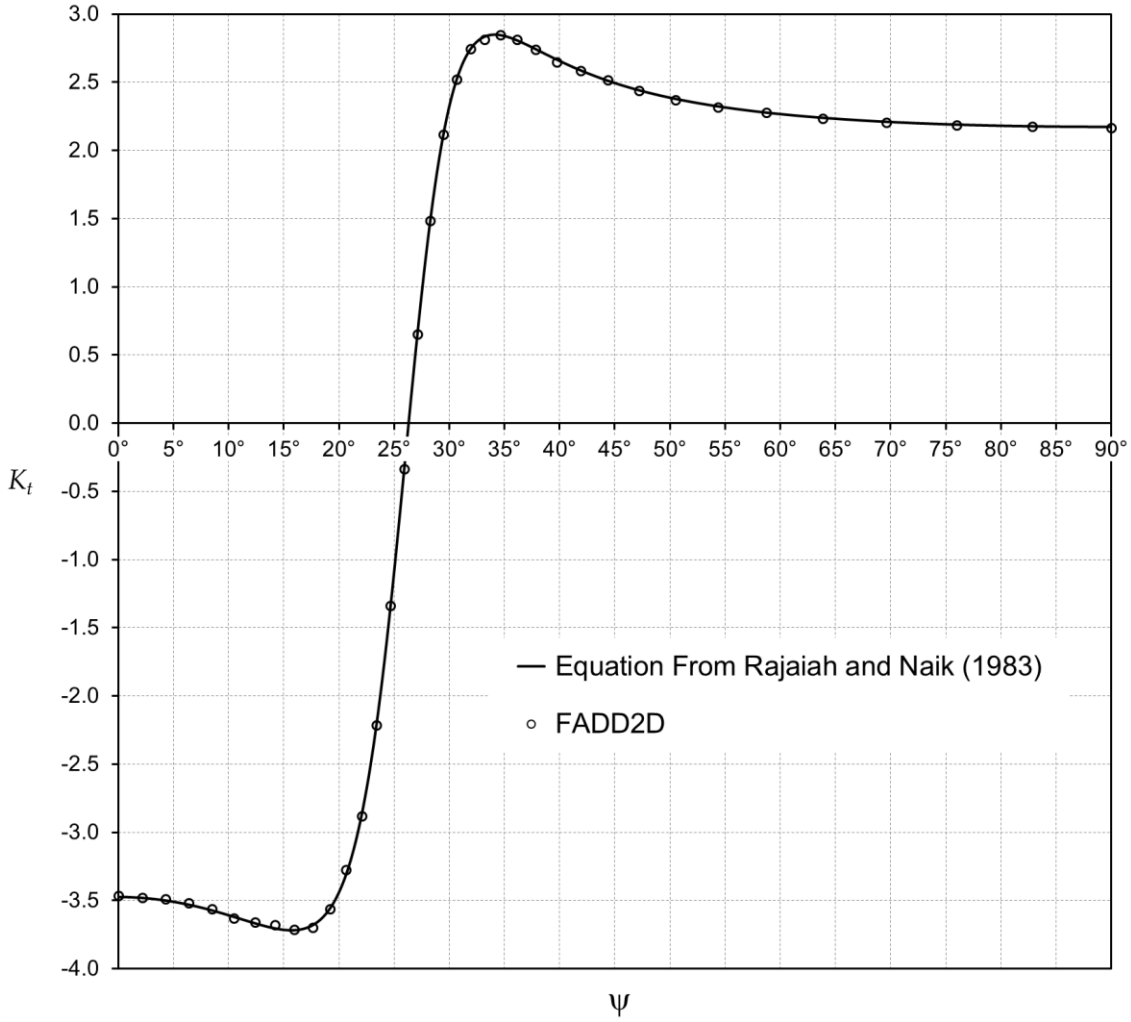

(b)

Figure 4: *Quasi-rectangular hole with shape parameters $\varepsilon = -0.0876$ and $\alpha = 0.5269$ under a remote biaxial loading $\sigma_x:\sigma_y = 1:-1$. (a) Hole shape. (b) Comparison of K_t distribution around one-quarter of the hole boundary, as computed by the method of Rajaiah and Naik (1983) and also by the FADD2D boundary element analysis code of Chang and Mear (1995).*

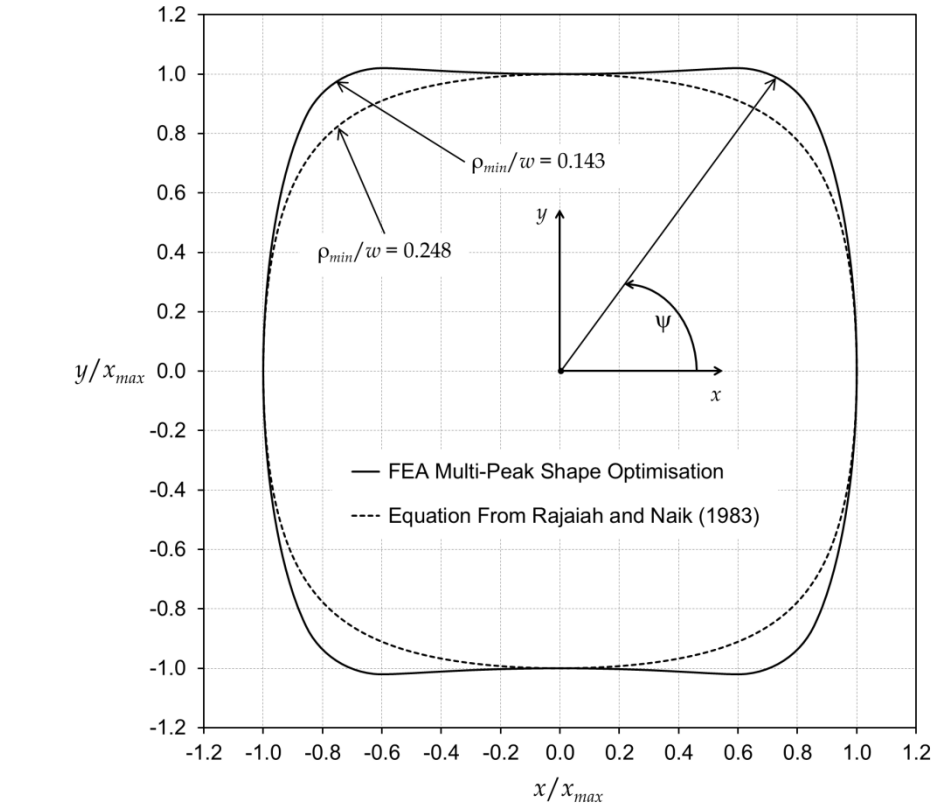

(a)

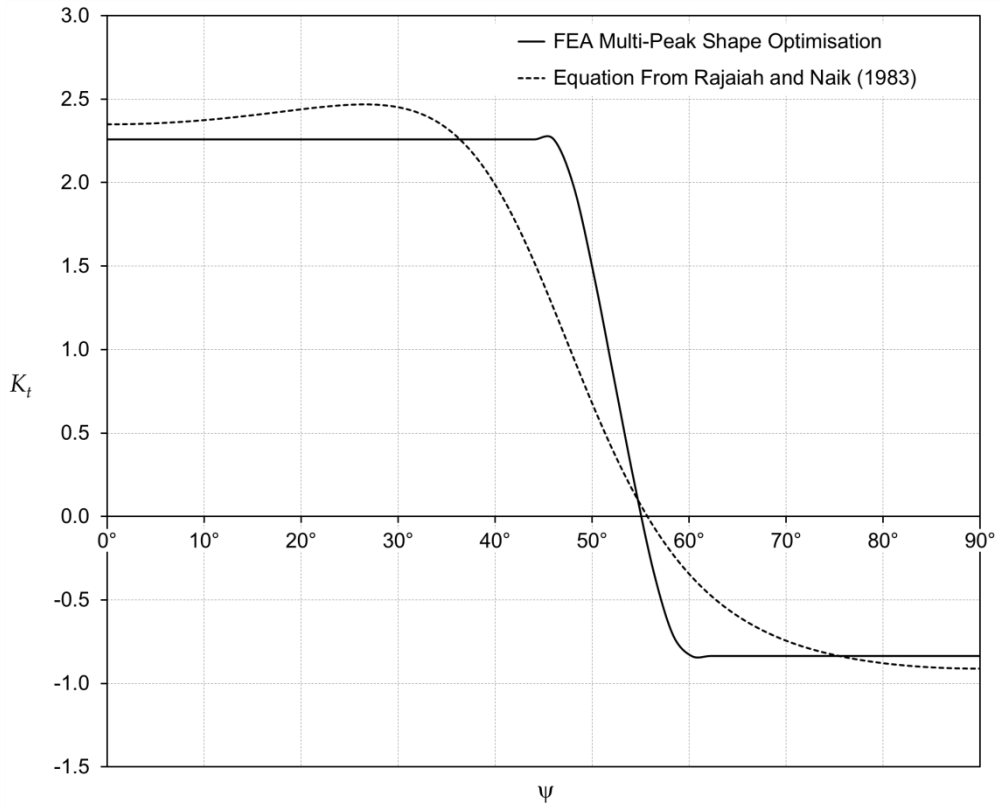

(b)

Figure 5: *Quasi-square 1:1 holes in a plate subject to remote uniaxial loading σ_x:σ_y = 0:1 obtained using method of Rajaiah and Naik (1983), with shape parameters ε = –0.0545 and α = 1, and from free-form FEA-based multiple stress peak shape optimisation. (a) Hole shapes. (b) K_t distributions around one-quarter of hole boundary.*

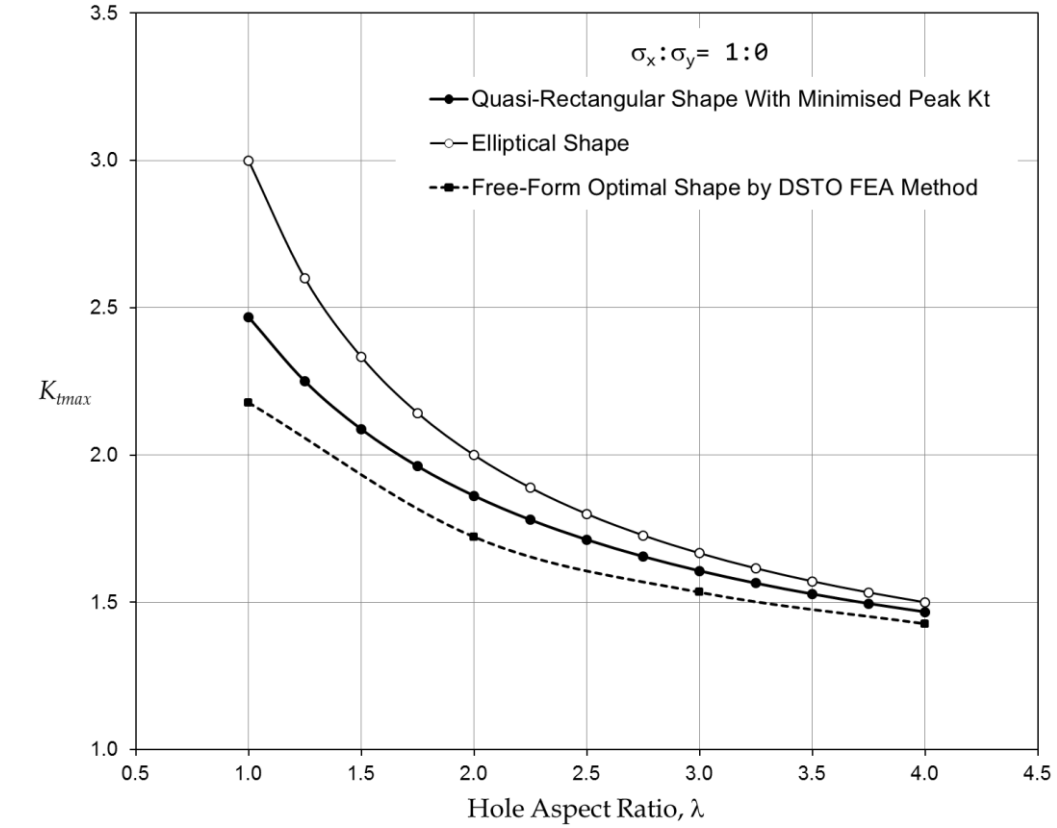

(a)

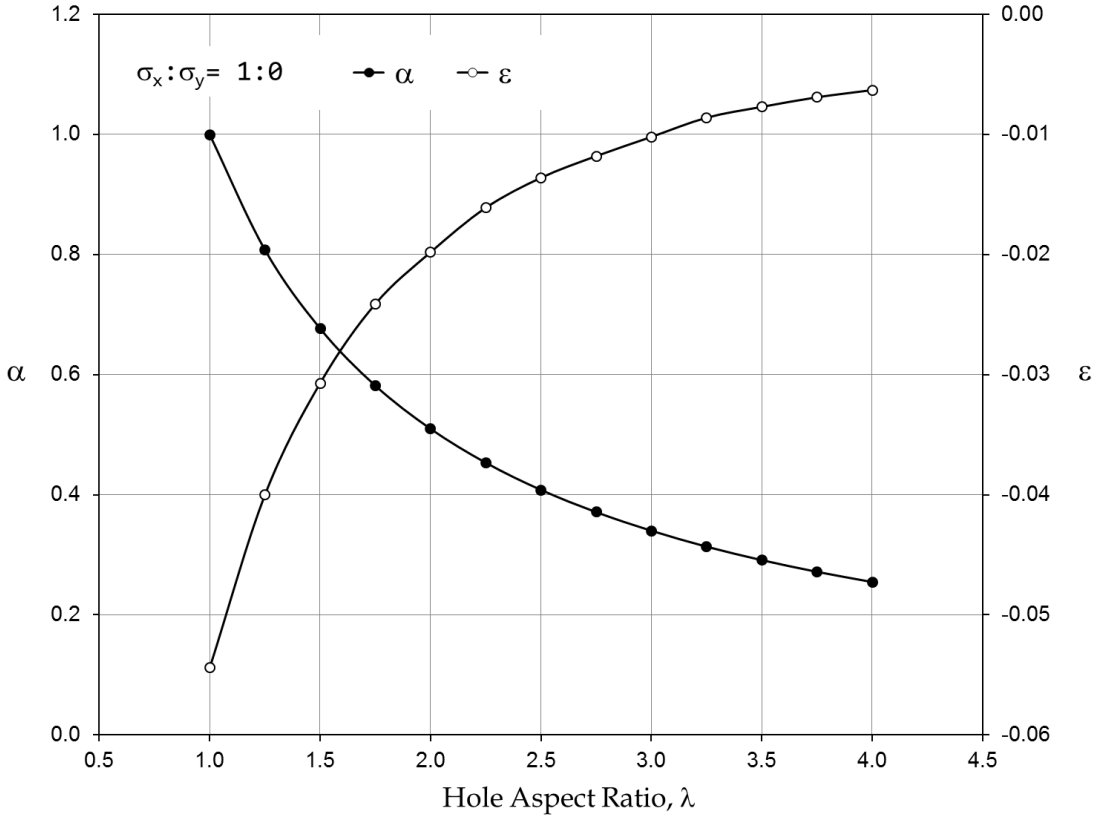

(b)

Figure 6: *(a) K_t values for stress-minimised quasi-rectangular holes, elliptical holes and FEA-optimised holes of various aspect ratios in an infinite plate under a uniaxial remote loading of σ_x:σ_y = 1:0. (b) Corresponding shape parameters α and ε for the quasi-rectangular holes.*

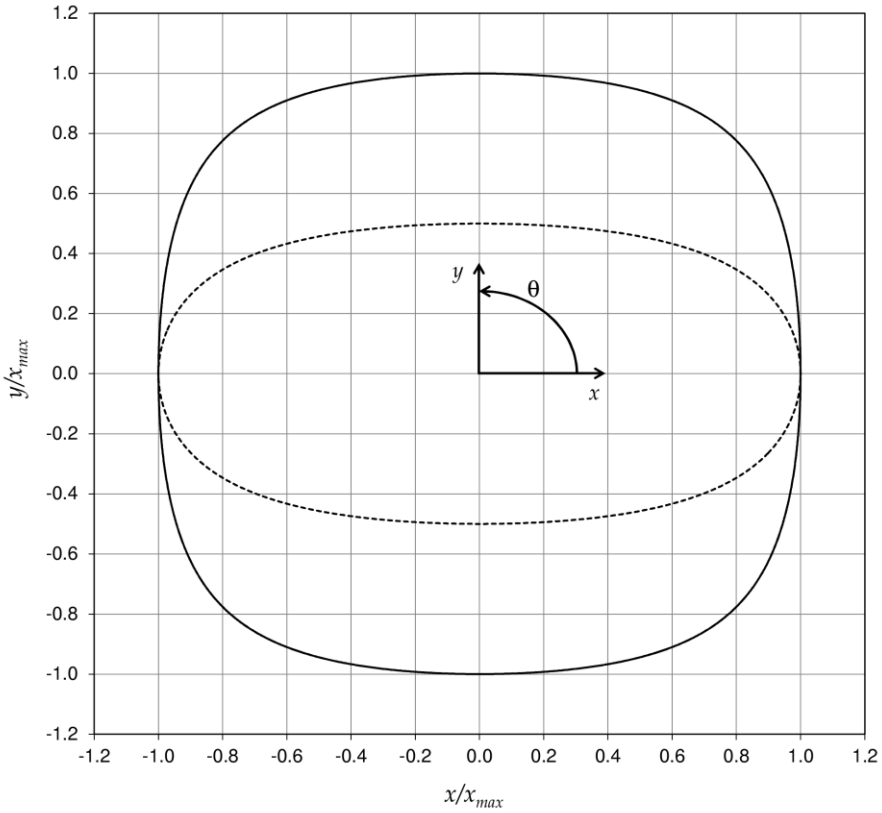

(a)

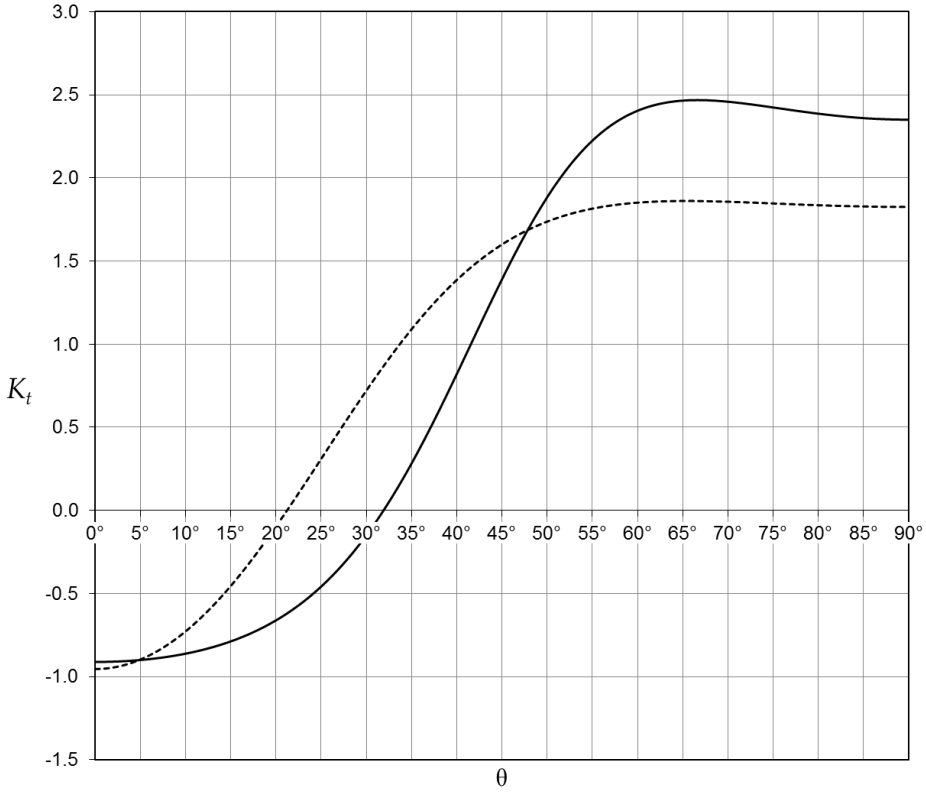

(b)

Figure 7: *Example quasi-rectangular holes with minimised peak K_t for hole aspect ratios of λ = 1 (solid line) and λ = 2 (dashed line) in an infinite plate under a uniaxial remote loading of σ_x:σ_y = 1:0. (a) Shapes. (b) K_t distributions around the hole boundaries.*

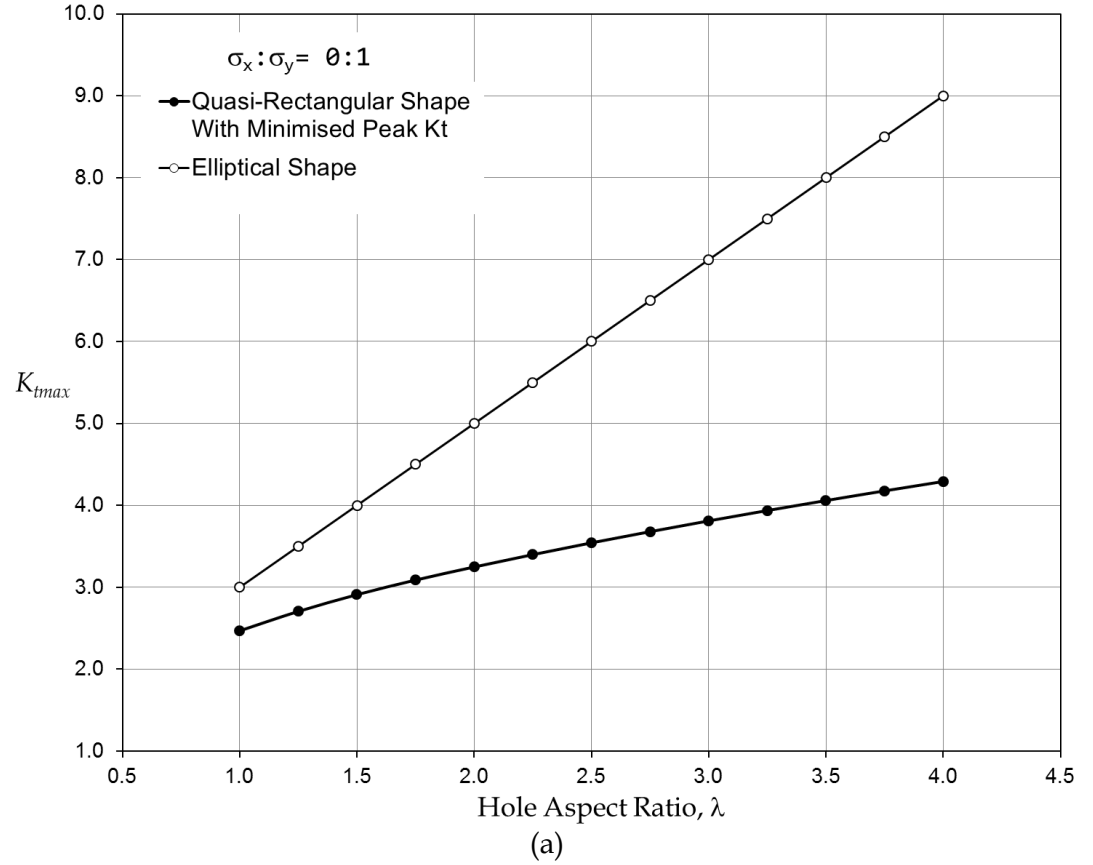

(a)

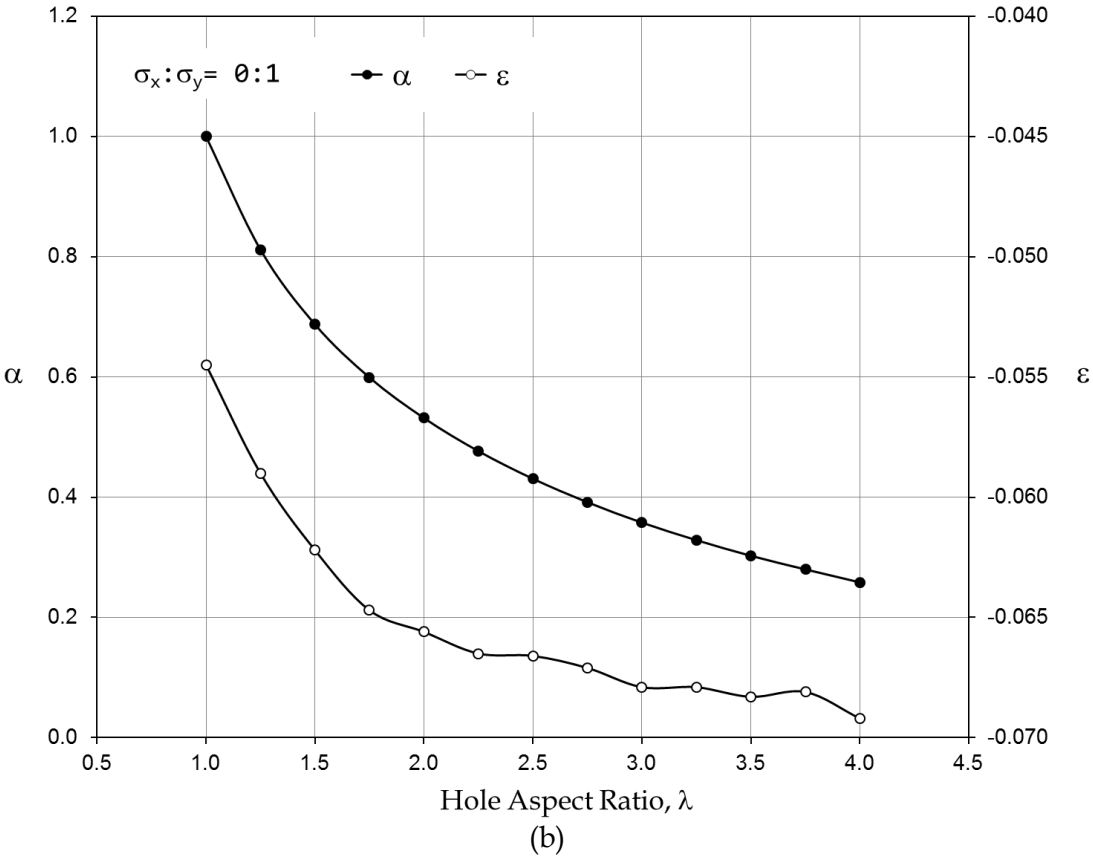

(b)

Figure 8: *(a) K_t values for stress-minimised quasi-rectangular holes and for elliptical holes of various hole aspect ratios in an infinite plate under a uniaxial remote loading of σ_x:σ_y = 0:1. (b) Corresponding shape parameters α and ε for the quasi-rectangular holes.*

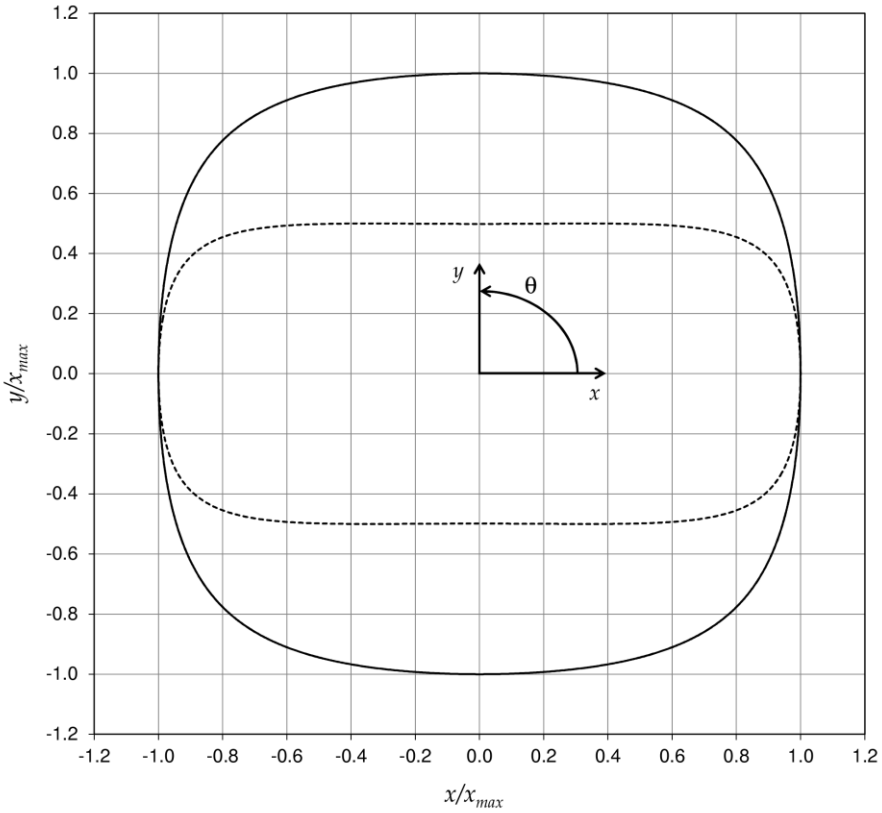

(a)

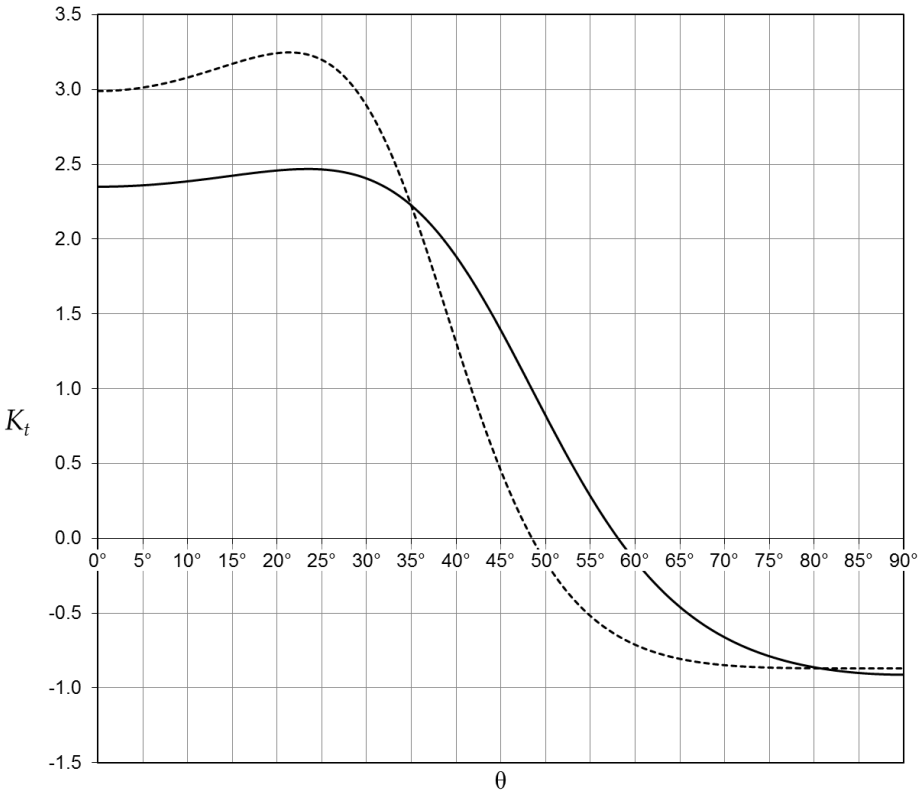

(b)

Figure 9: *Example quasi-rectangular holes with minimised peak K_t for hole aspect ratios of λ = 1 (solid line) and λ = 2 (dashed line) in an infinite plate under a uniaxial remote loading of σ_x:σ_y = 0:1. (a) Shapes. (b) K_t distributions around the hole boundaries.*

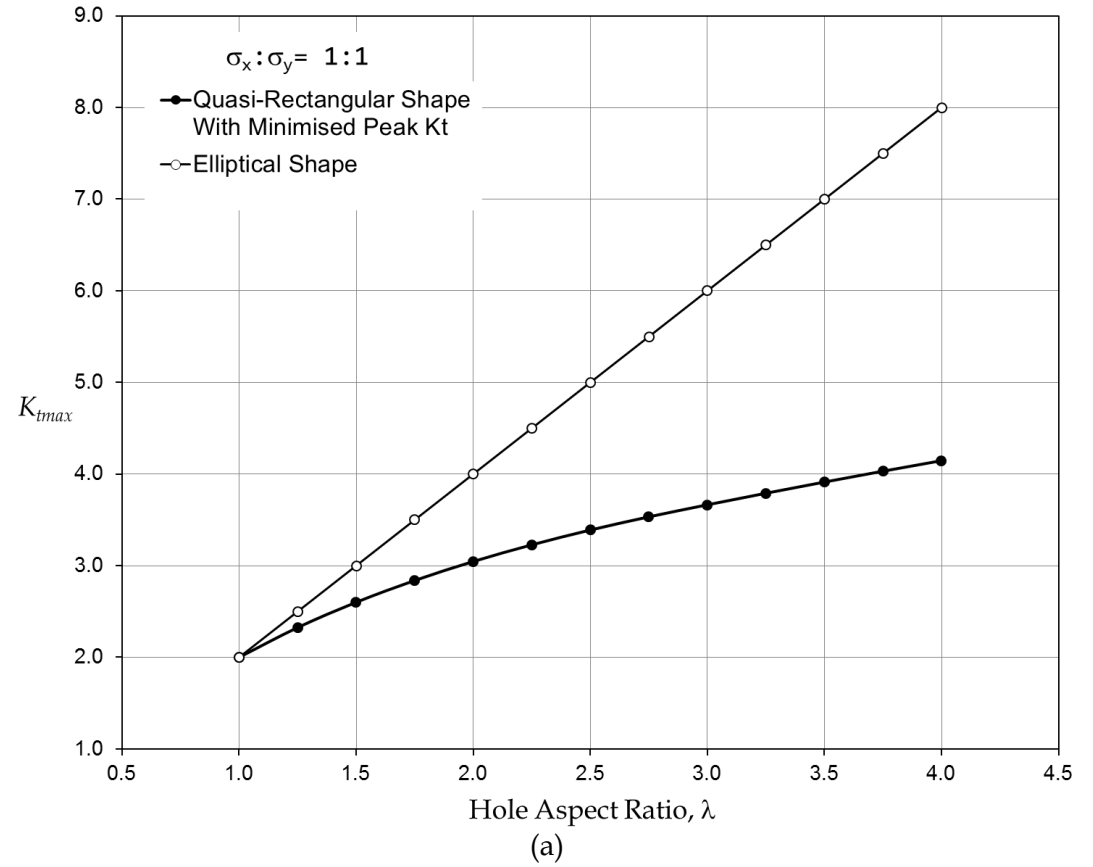

(a)

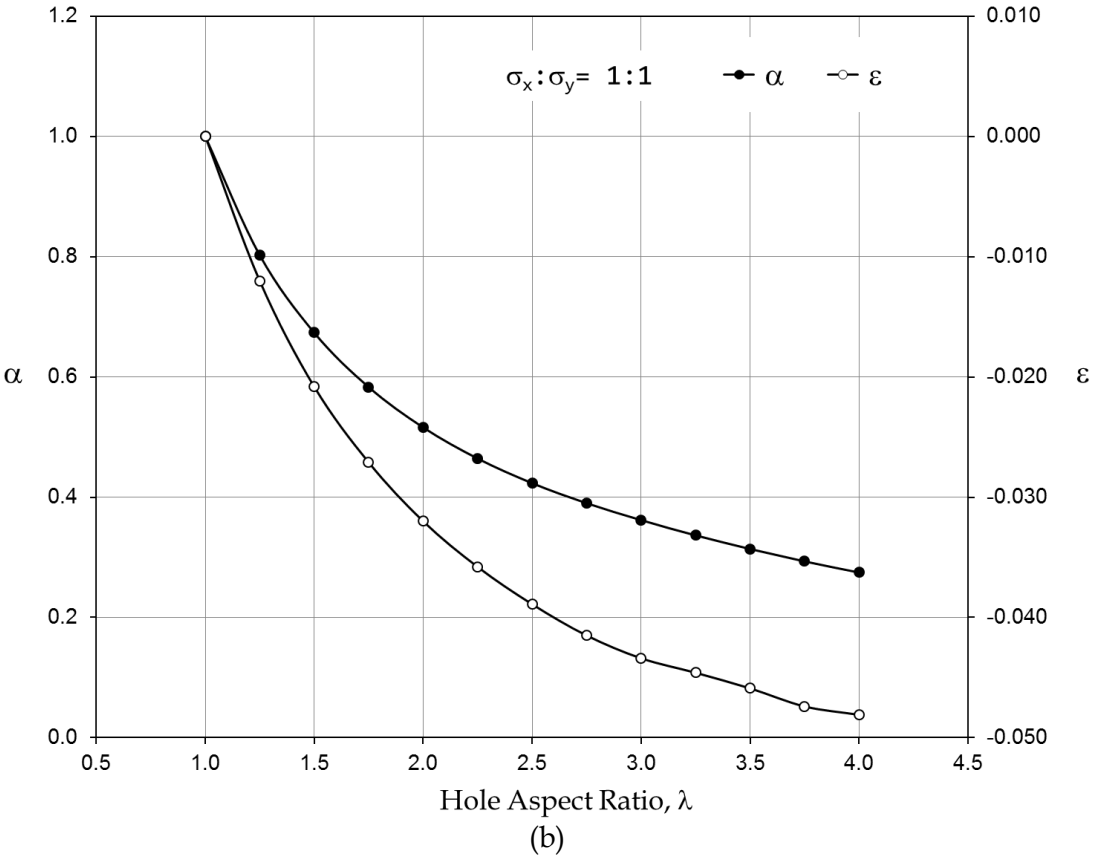

(b)

Figure 10: *(a) K_t values for stress-minimised quasi-rectangular holes and for elliptical holes of various hole aspect ratios in an infinite plate under an equibiaxial remote loading of σ_x:σ_y = 1:1. (b) Corresponding shape parameters α and ε for the quasi-rectangular holes.*

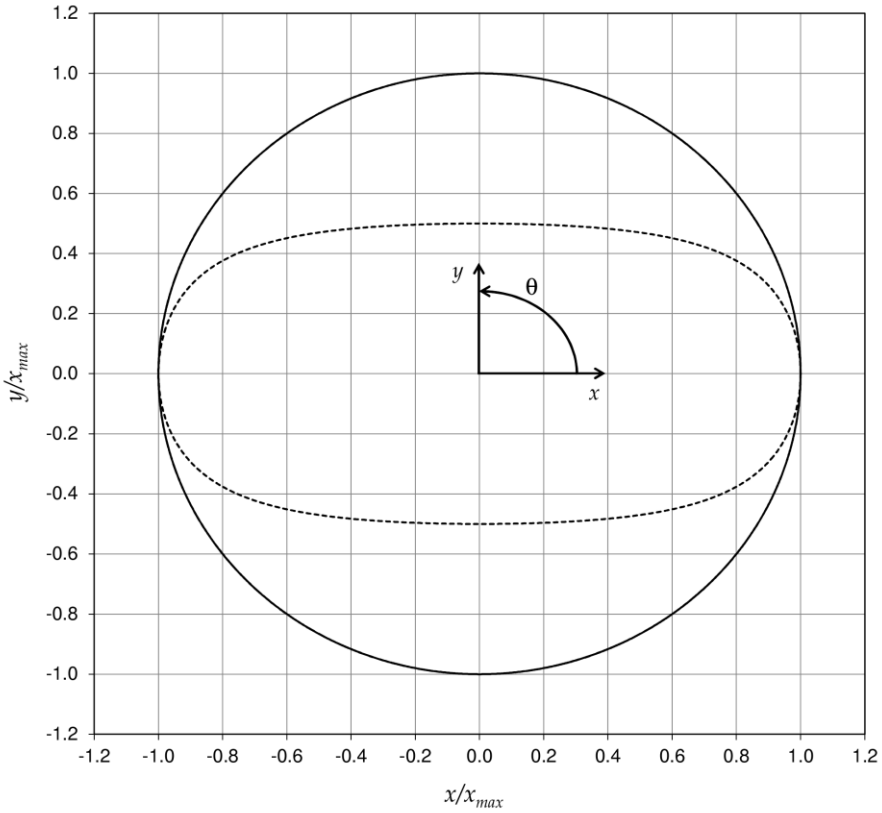

(a)

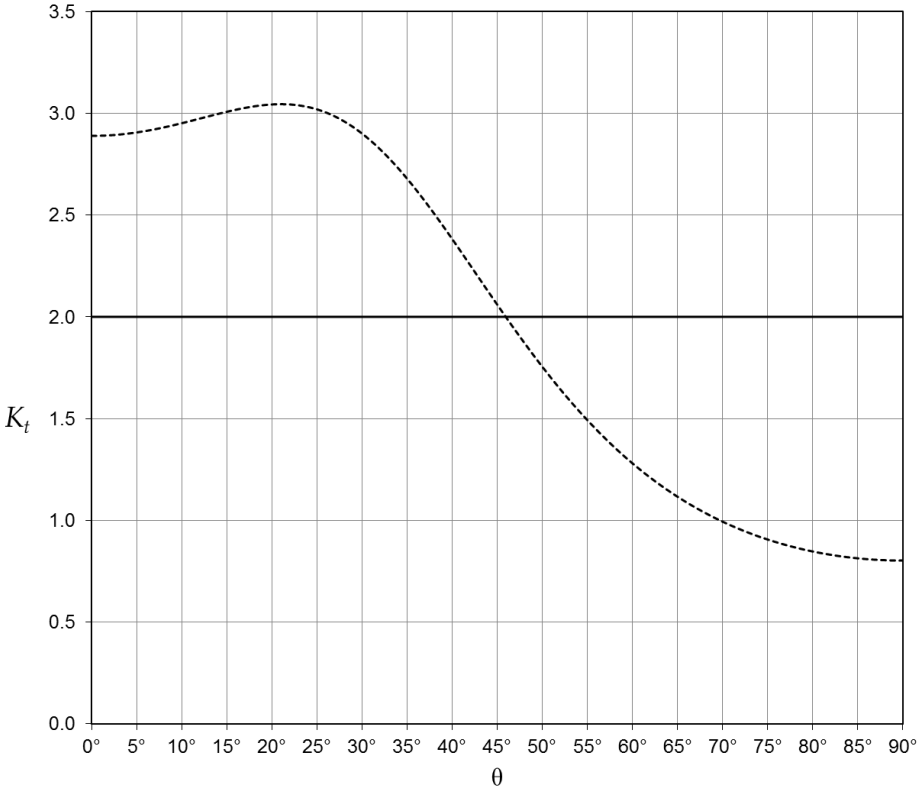

(b)

Figure 11: *Example quasi-rectangular holes with minimised peak K_t for hole aspect ratios of λ = 1 (solid line) and λ = 2 (dashed line) in an infinite plate under a biaxial remote loading of σ_x:σ_y = 1:1. (a) Shapes. (b) K_t distributions around the hole boundaries.*

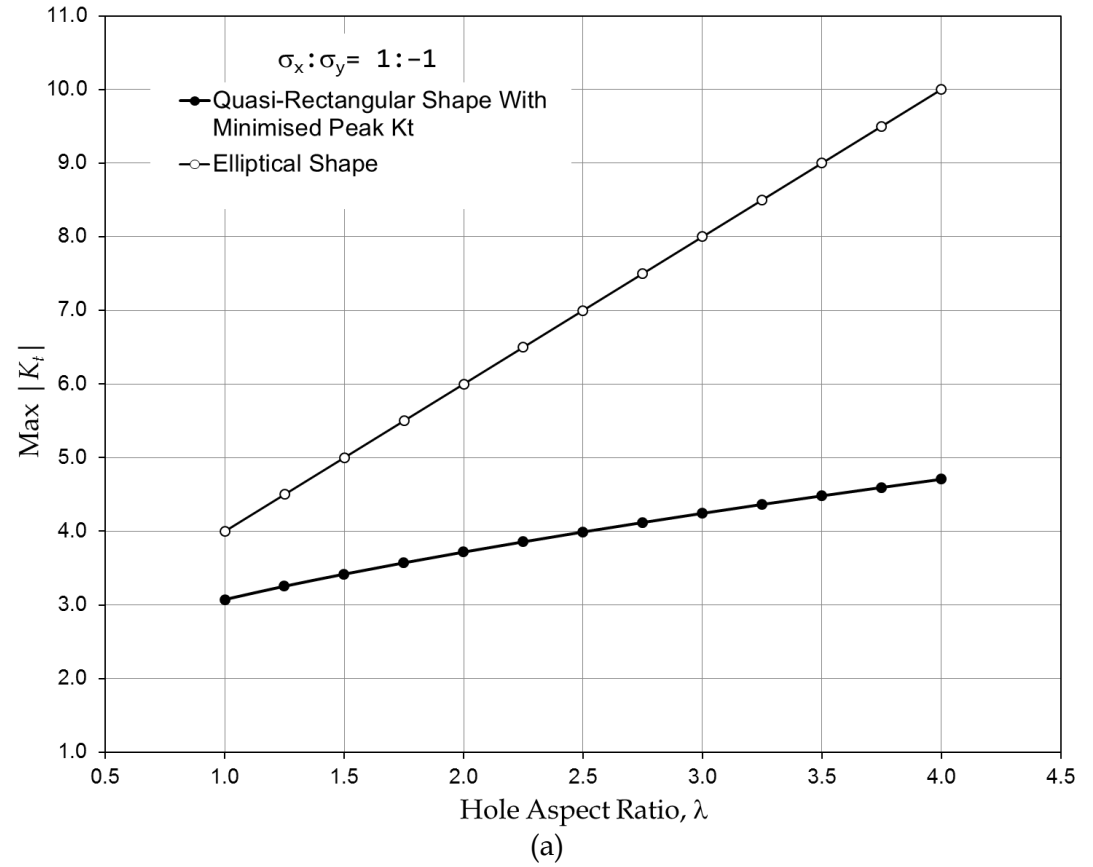

Figure 12: *(a) K_t values for stress-minimised quasi-rectangular holes and for elliptical holes of various hole aspect ratios in an infinite plate under a biaxial remote loading of σ_x:σ_y = 1:–1. (b) Corresponding shape parameters α and ε for the quasi-rectangular holes.*

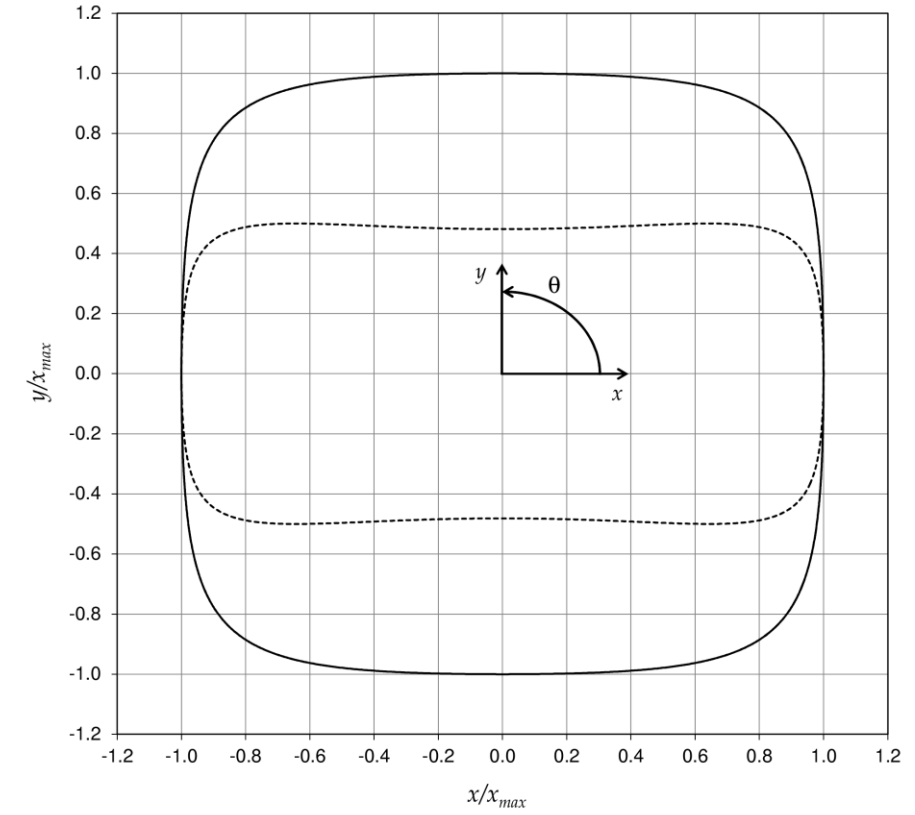

(a)

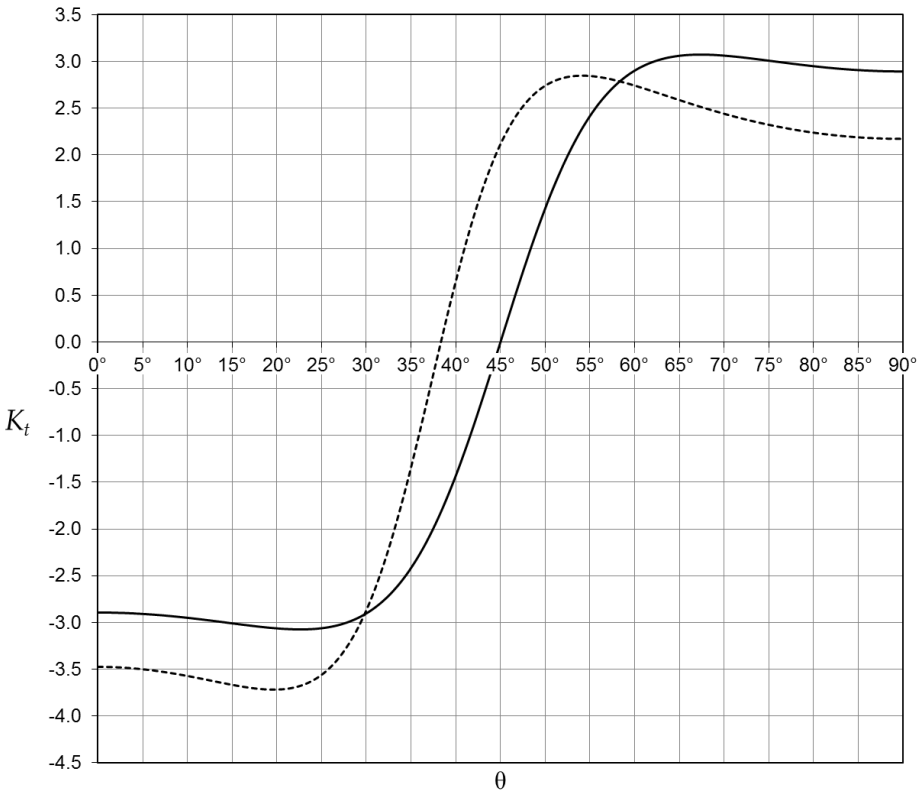

(b)

Figure 13: *Example quasi-rectangular holes with minimised peak K_t for hole aspect ratios of $\lambda = 1$ (solid line) and $\lambda = 2$ (dashed line) in an infinite plate under a biaxial remote loading of $\sigma_x:\sigma_y = 1:-1$. (a) Shapes. (b) K_t distributions around the hole boundaries.*

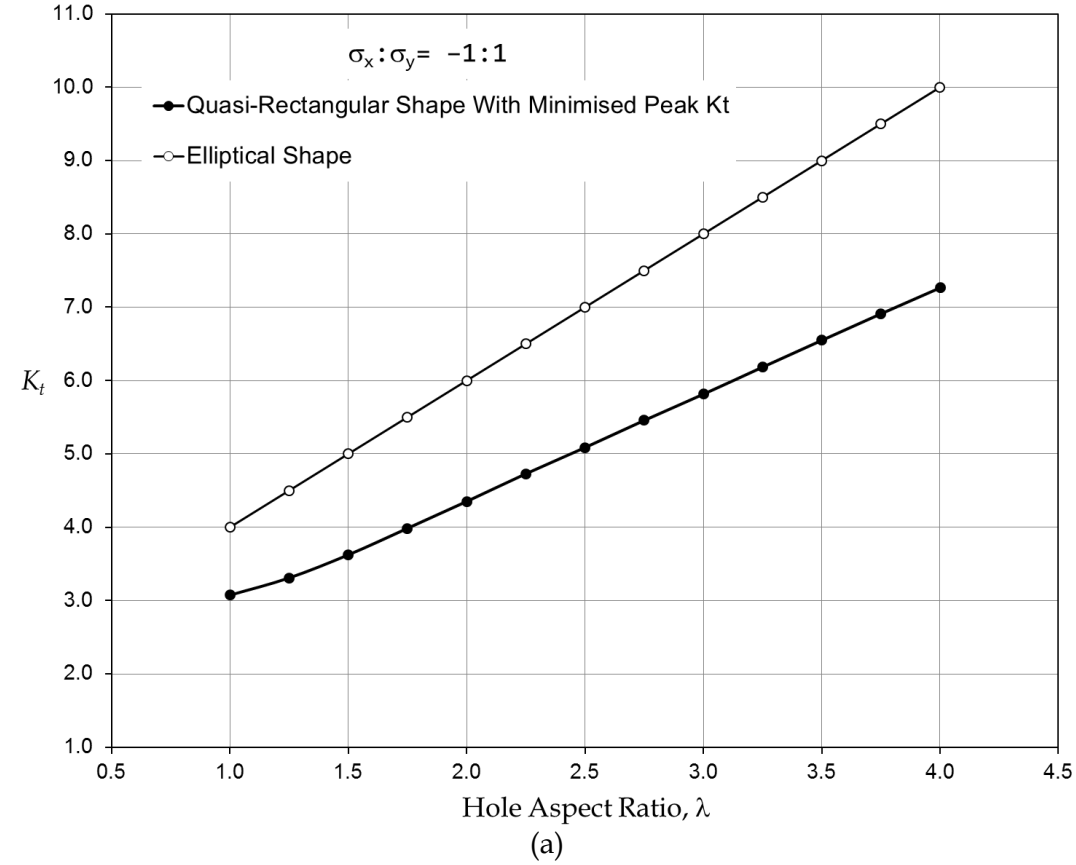

(a)

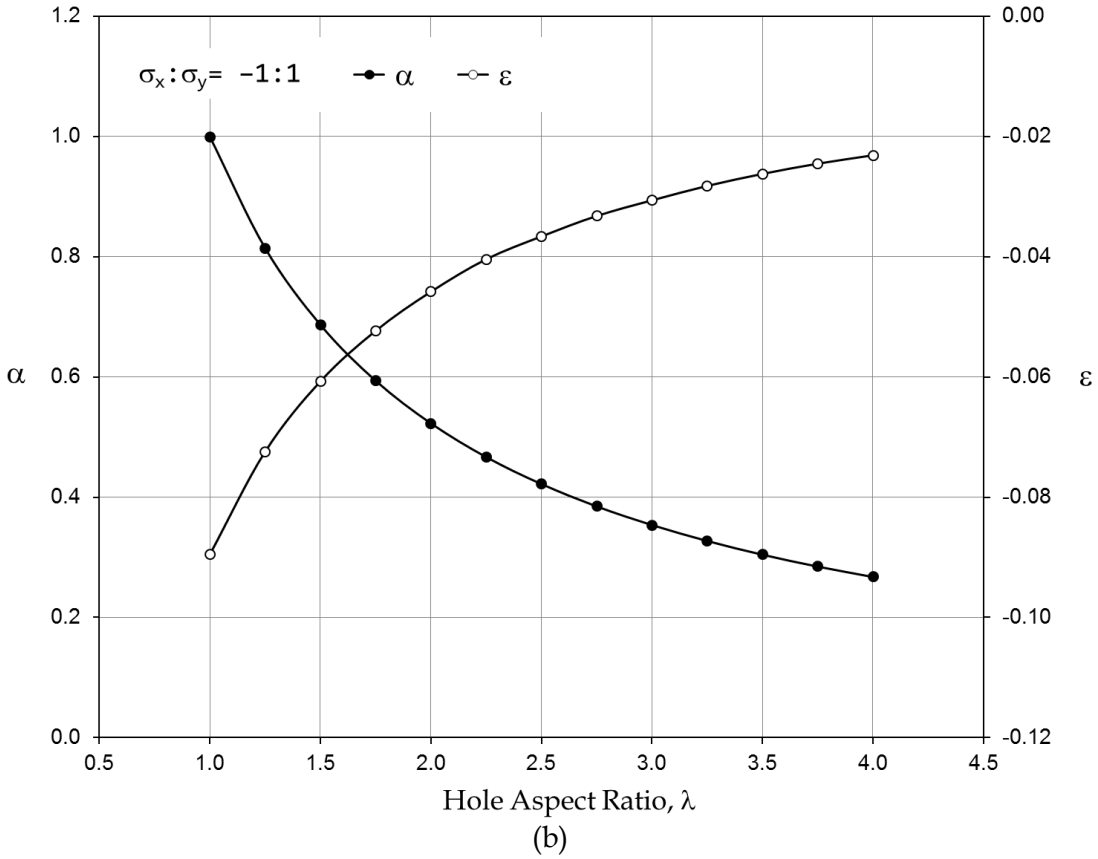

(b)

Figure 14: *(a) K_t values for stress-minimised quasi-rectangular holes and for elliptical holes of various hole aspect ratios in an infinite plate under a biaxial remote loading of σ_x:σ_y = –1:1. (b) Corresponding shape parameters α and ε for the quasi-rectangular holes.*

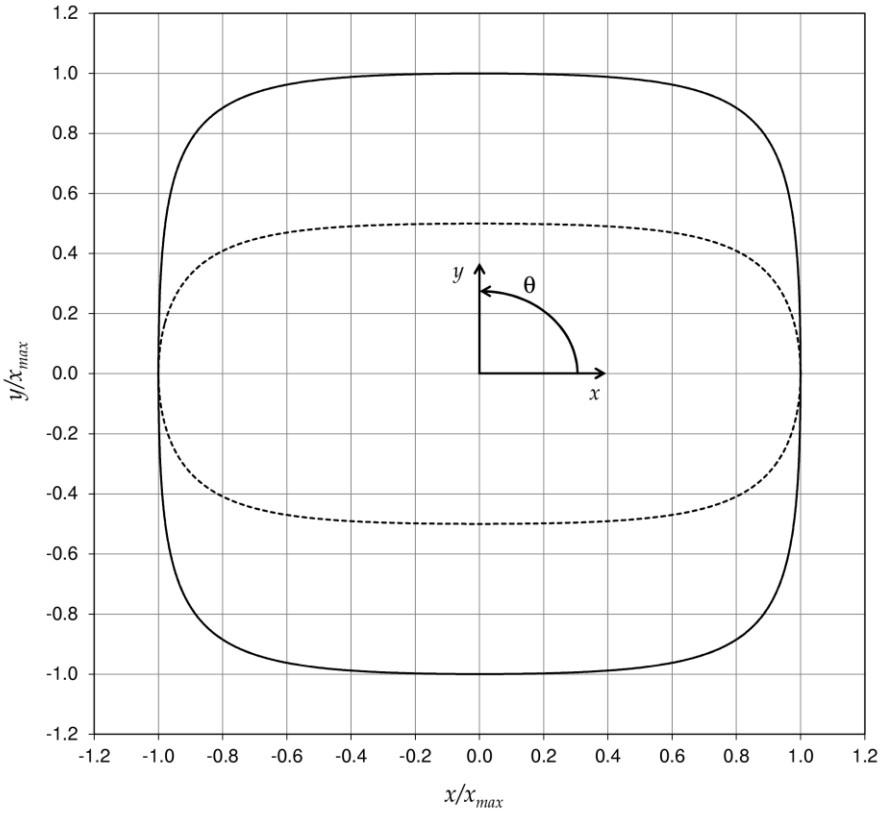

(a)

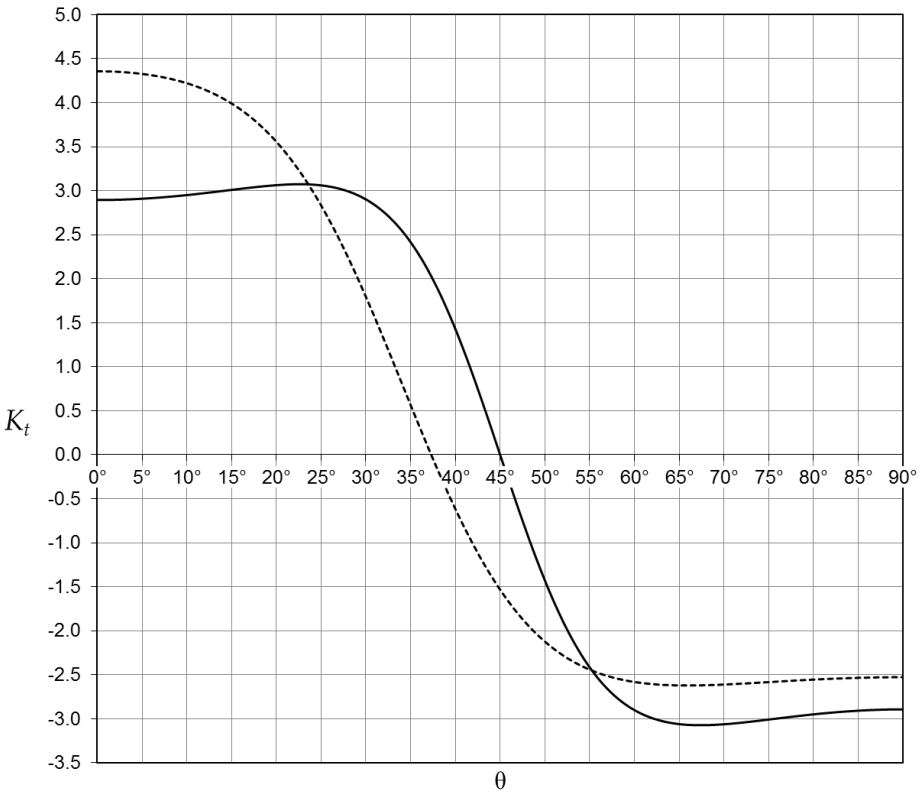

(b)

Figure 15: *Example quasi-rectangular holes with minimised peak K_t for hole aspect ratios of $\lambda = 1$ (solid line) and $\lambda = 2$ (dashed line) in an infinite plate under a biaxial remote loading of $\sigma_x:\sigma_y = -1:1$. (a) Shapes. (b) K_t distributions around hole boundaries.*

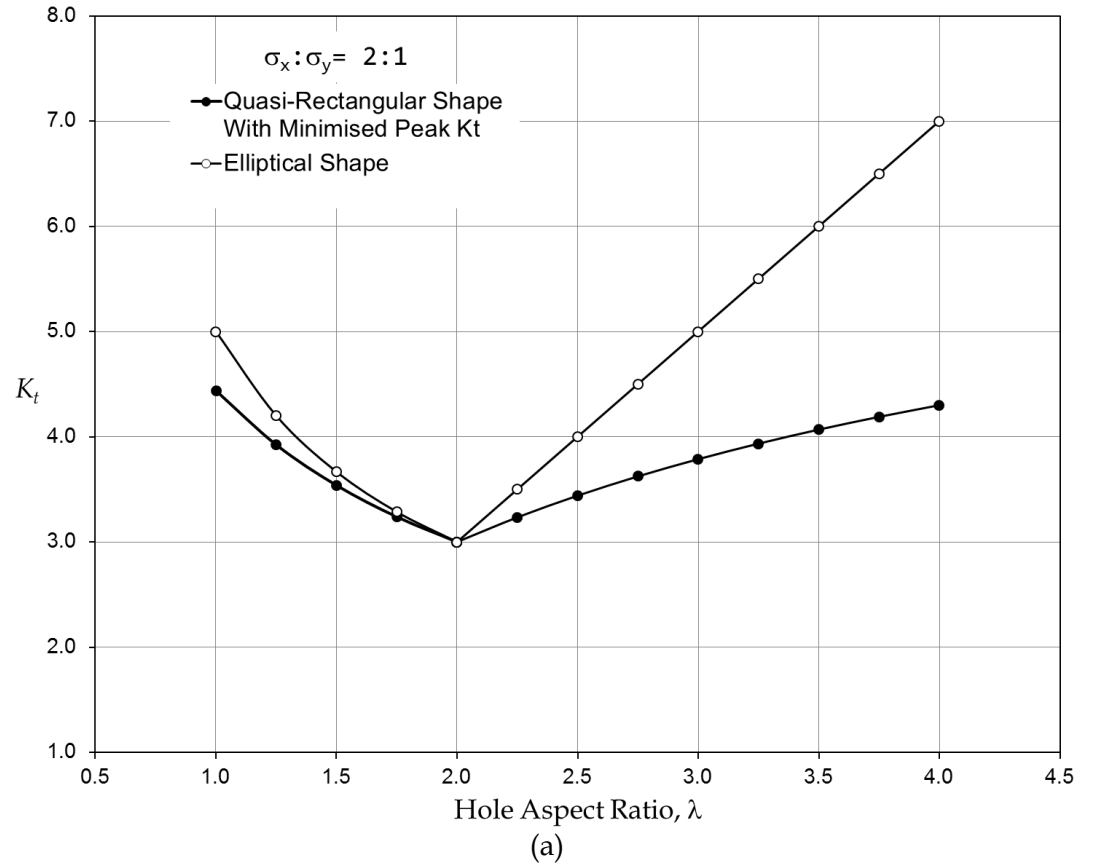

(a)

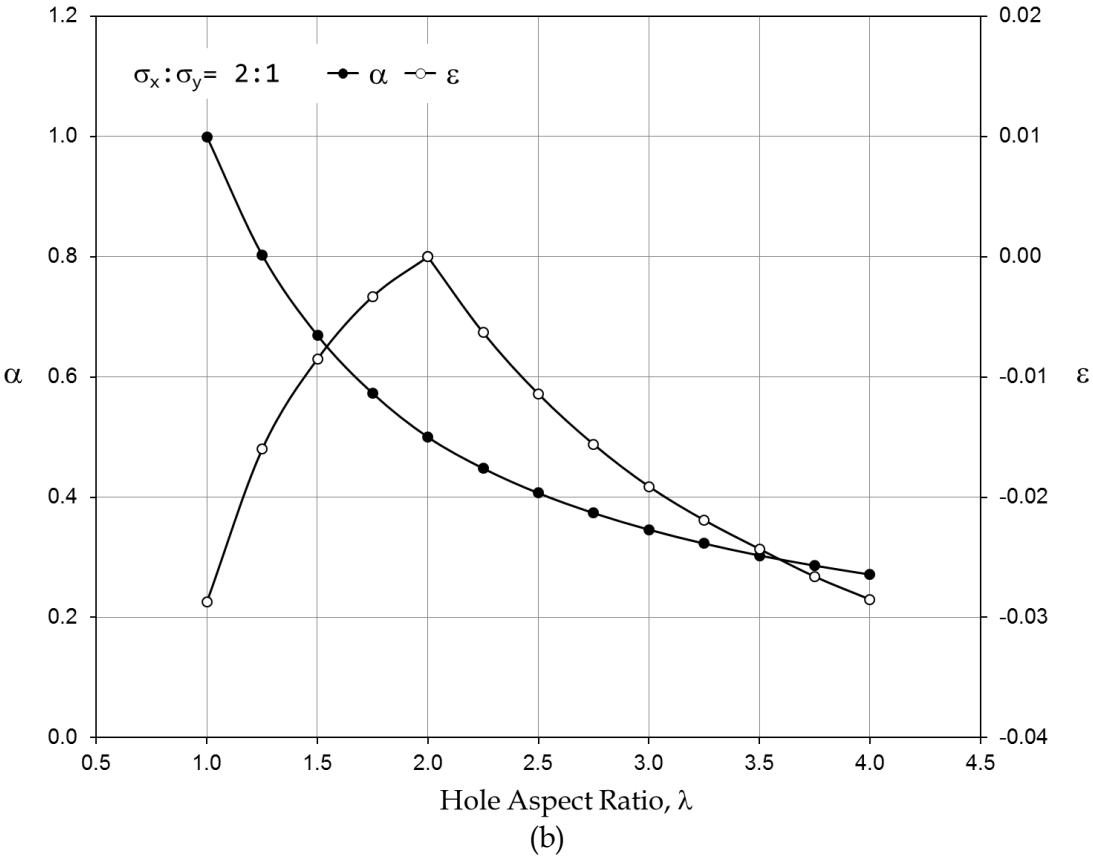

(b)

Figure 16: *(a) K_t values for stress-minimised quasi-rectangular holes and for elliptical holes of various hole aspect ratios in an infinite plate under a biaxial remote loading of σ_x:σ_y = 2:1. (b) Corresponding shape parameters α and ε for the quasi-rectangular holes.*

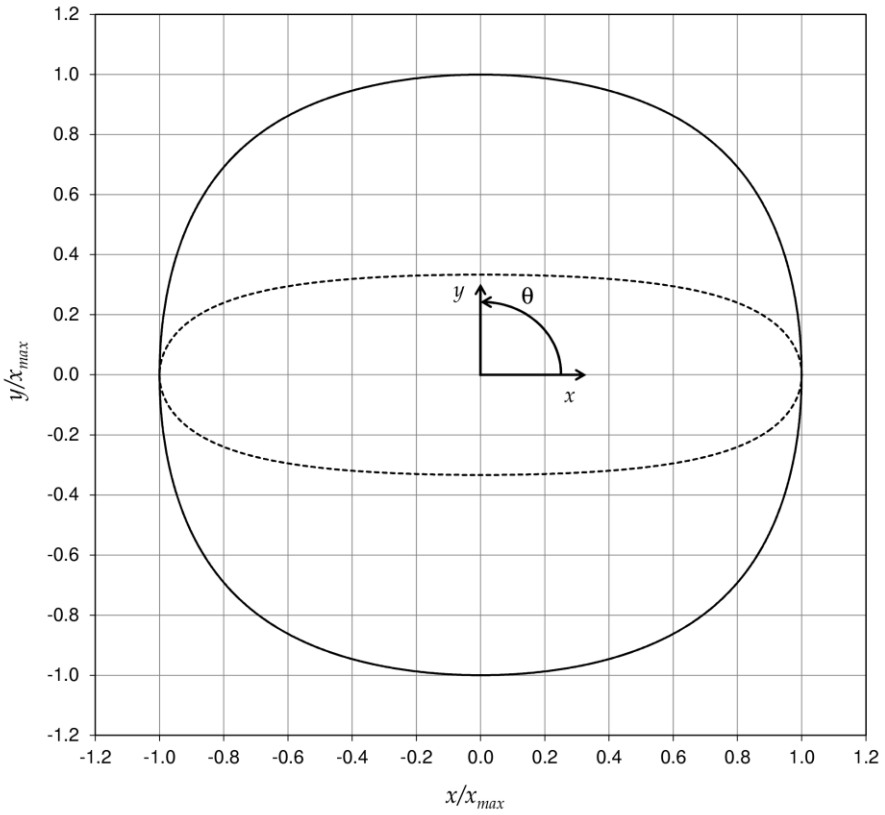

(a)

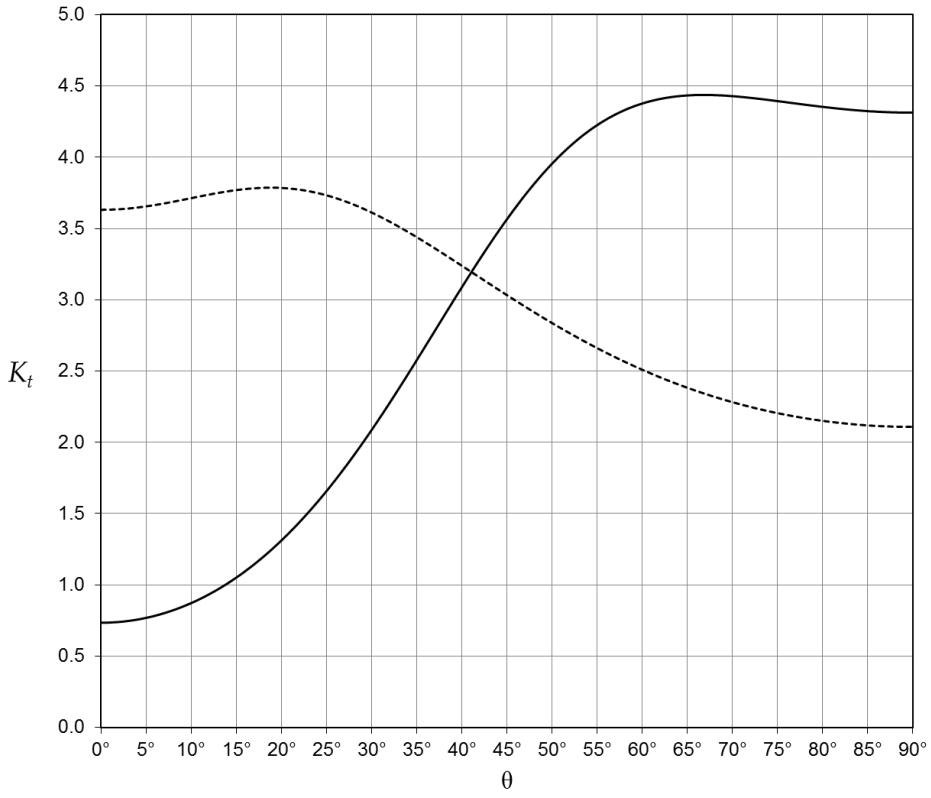

(b)

Figure 17: *Example quasi-rectangular holes with minimised peak K_t for hole aspect ratios of λ = 1 (solid line) and λ = 3 (dashed line) in an infinite plate under a biaxial remote loading of σ_x:σ_y = 2:1. (a) Shapes. (b) K_t distributions around hole boundaries.*

Appendix A:
Functions for computing shapes and stress distributions for quasi-rectangular holes using Excel VBA

What follows is the VBA source listing of the various functions that were used to implement the method of Rajaiah and Naik (1983) for computing shapes and distributions of tangential stress for quasi-rectangular holes in biaxially-loaded infinite plates. The functions associated with computing similar closed-form analytical solutions for circular and elliptical holes are also included for completeness, as they can provide useful points of comparison in some situations. It is hoped that others will find this small set of utility functions to be helpful in their own work.

```
Option Explicit

'=====================================================================

Function RofC(r, eta, alpha, tdeg As Double) As Double

' Compute the radius of curvature of the quasi-rectangular shape.

Dim Pi, theta, x1, x2, y1, y2, t, sint, cost, sin3t, cos3t As Double
Dim Numer, Denom As Double

Pi = 4 * Atn(1)

t = tdeg * Pi / 180
sint = Sin(t)
cost = Cos(t)
sin3t = Sin(3 * t)
cos3t = Cos(3 * t)

x1 = r * (-sint - 3 * eta * sin3t)
x2 = r * (-cost - 9 * eta * cos3t)
y1 = r * (alpha * cost - 3 * eta * cos3t)
y2 = r * (-alpha * sint + 9 * eta * sin3t)

Numer = (x1 ^ 2 + y1 ^ 2) ^ 1.5
Denom = x1 * y2 - y1 * x2

If Denom = 0# Then
  ' Prevent an infinite radius of curvature (straight line)
  ' from affecting the calculations.
  RofC = r * 1000000#
Else
  RofC = Abs(Numer / Denom)
End If

End Function

'=====================================================================

Function Xval(r, eta, alpha, thetadeg As Double) As Double

' Compute X-coordinate of shape.

Dim Pi, theta As Double

Pi = 4 * Atn(1)

theta = thetadeg * Pi / 180
```

```
Xval = r * (Cos(theta) + eta * Cos(3 * theta))

End Function

'=====================================================================

Function Yval(r, eta, alpha, thetadeg As Double) As Double

' Compute Y-coordinate of shape.

Dim theta, Pi As Double

Pi = 4 * Atn(1)

theta = thetadeg * Pi / 180

Yval = r * (alpha * Sin(theta) - eta * Sin(3 * theta))

End Function

'=====================================================================

Function Kt(eta, alpha, Sx, Sy, thetadeg As Double) As Double

' Tangential stress around hole boundary when the plate is subjected
' to uniform tension stresses Sx and Sy.
'
' Rajaiah K, Naik NK. Hole shapes with minimum stress concentration
' in infinite isotropic plates using conformal transformation.
' ISME Journal of Engineering Design, Vol 1, No 1, April 1983,
' pp 15-19.

Dim Pi, theta, Ktx, Kty, a, b, C2 As Double
Dim cost, sint, cos3t, sin3t, alphap1 As Double

Pi = 4 * Atn(1)

theta = thetadeg * Pi / 180

cost = Cos(theta)
sint = Sin(theta)
cos3t = Cos(3 * theta)
sin3t = Sin(3 * theta)
alphap1 = alpha + 1

a = alpha * cost - 3 * eta * cos3t
b = sint + 3 * eta * sin3t

C2 = a ^ 2 + b ^ 2

' Tangential stress around hole for tension aligned with x-axis.

Ktx = (b ^ 2 / C2) + (1 / C2) * (alpha * (-a * cost _
      + 2 * b * sint) - eta * (4 * a * alpha * cost / alphap1 _
      - 3 * a * cos3t + 2 * b * (-2 * alpha * sint / alphap1 _
      + 3 * sin3t)) _
      - 8 * eta ^ 2 * alpha / alphap1 ^ 2 * (a * cost - b * sint))

' Tangential stress around hole for tension aligned with y-axis.

Kty = (a ^ 2 / C2) + (1 / C2) * (2 * a * cost _
      - b * sint + eta * (2 * a * (2 * cost / alphap1 _
      + 3 * cos3t) - 4 * b * sint / alphap1 _
      - 3 * b * sin3t) _
      + 8 * eta ^ 2 / alphap1 ^ 2 * (a * cost - b * sint))
```

```
Kt = Ktx * Sx + Kty * Sy

End Function

'=====================================================================

Function XvalCircle(r, thetadeg As Double) As Double

' Compute X-coordinate of shape.

Dim theta, Pi As Double

Pi = 4 * Atn(1)

theta = thetadeg * Pi / 180

XvalCircle = r * (Cos(theta))

End Function

'=====================================================================

Function YvalCircle(r, thetadeg As Double) As Double

' Compute Y-coordinate of shape.

Dim theta, Pi As Double

Pi = 4 * Atn(1)

theta = thetadeg * Pi / 180

YvalCircle = r * Sin(theta)

End Function

'=====================================================================

Function KtCircle(Sx, Sy, thetadeg As Double) As Double

' Tangential stress around boundary of a circular hole in a plate
' when the plate is subjected to uniform tension stresses Sx and Sy.

Dim Pi, theta, Ktx, Kty As Double

Pi = 4 * Atn(1)

theta = thetadeg * Pi / 180

' Tangential stress around hole for tension aligned with x-axis.

Ktx = (1 - 2 * Cos(2 * theta))

' Tangential stress around hole for tension aligned with y-axis.

Kty = (1 - 2 * Cos(2 * (theta - Pi / 2)))

KtCircle = Ktx * Sx + Kty * Sy

End Function

'=====================================================================

Function KtEllipse(Sx, Sy, a, b, thetadeg As Double) As Double

' Tangential stress around boundary of an elliptical hole in a plate
' when the plate is subjected to uniform tension stresses Sx and Sy.
```

```
Dim Pi, theta, m, m2, cos2t, Ktx, Kty As Double

Pi = 4 * Atn(1)

theta = thetadeg * Pi / 180

m = (a - b) / (a + b)
m2 = m ^ 2
cos2t = Cos(2 * theta)

' Tangential stress around hole for tension aligned with x-axis.

Ktx = (2 * m + 1 - 2 * cos2t - m2) / (m2 - 2 * m * cos2t + 1)

' Tangential stress around hole for tension aligned with y-axis.

Kty = (-2 * m + 1 + 2 * cos2t - m2) / (m2 - 2 * m * cos2t + 1)

KtEllipse = Ktx * Sx + Kty * Sy

End Function

'=====================================================================

Function XvalEllipse(a, thetadeg As Double) As Double

' Compute X-coordinate of elliptical shape with semimajor axis
' length a.

Dim Pi, theta As Double

Pi = 4 * Atn(1)

theta = thetadeg * Pi / 180

XvalEllipse = a * (Cos(theta))

End Function

'=====================================================================

Function YvalEllipse(b, thetadeg As Double) As Double

' Compute Y-coordinate of elliptical shape with semiminor axis
' length b.

Dim Pi, theta As Double

Pi = 4 * Atn(1)

theta = thetadeg * Pi / 180

YvalEllipse = b * Sin(theta)

End Function

'=====================================================================

Function Stteum(a, b, S, thetadeg, gammadeg As Double) As Double

' Compute tangential stress at the edge of an elliptical hole in an
' infinite plate due to a remote uniaxial stress field of intensity
' S acting at an angle gamma.
'
' NI Muskhelishvili. Some basic problems of the mathematical theory
' of elasticity. Third Edition, 1953, P Noordhoff Ltd, Groningen,
```

```
' Holland.

Dim Pi, theta, gamma, m As Double

Pi = 4 * Atn(1)

theta = thetadeg * Pi / 180
gamma = gammadeg * Pi / 180

m = (a - b) / (a + b)

Stteum = S * (1 - m ^ 2 + 2 * m * Cos(2 * gamma) _
              - 2 * Cos(2 * (theta - gamma))) _
            / (1 - 2 * m * Cos(2 * theta) + m ^ 2)

End Function

'=====================================================================

Function Sttebm(Sx, Sy, a, b, thetadeg As Double) As Double

' Compute tangential stress around the edge of an elliptical hole in
' an infinite plate due to a remote biaxial stress field of intensity
' Sx and Sy. Muskhelishvili's equation is used.

Dim Stteux, Stteuy As Double

Stteux = Stteum(a, b, 1#, thetadeg, 0#)
Stteuy = Stteum(a, b, 1#, thetadeg, 90#)

Sttebm = Sx * Stteux + Sy * Stteuy

End Function

'=====================================================================

Function Sttesm(a, b, T, thetadeg As Double) As Double

' Compute tangential stress at the edge of an elliptical hole in an
' infinite plate due to a remote shear stress field of intensity T.
' Muskhelishvili's equation is used.

Dim Pi, theta As Double
Dim Stteu1, Stteu2 As Double

Stteu1 = Stteum(a, b, 1#, thetadeg, 45#)
Stteu2 = Stteum(a, b, 1#, thetadeg, 135#)

Sttesm = T * (Stteu1 - Stteu2)

End Function


'=====================================================================

Function Sttexytm(a, b, Sx, Sy, Txy, thetadeg As Double) As Double

' Compute tangential stress at the edge of an elliptical hole in an
' infinite plate due to remote direct stresses Sx and Sy and a
' remote shear stress Txy. Muskhelishvili's equation is applied to
' determine the equation.

Dim pi, theta, denom, m, m2, cos2t, sin2t As Double
Dim Sttx, Stty, Sttt As Double

pi = 4 * Atn(1)
```

```
theta = thetadeg * pi / 180

m = (a - b) / (a + b)
m2 = m ^ 2
cos2t = Cos(2 * theta)
sin2t = Sin(2 * theta)

Sttx = 1 - m2 + 2 * m - 2 * cos2t ' Component due to Sx
Stty = 1 - m2 - 2 * m + 2 * cos2t ' Component due to Sy
Sttt = -4 * sin2t                 ' Component due to Txy

denom = 1 - 2 * m * cos2t + m2

Sttexytm = (Sx * Sttx + Sy * Stty + Txy * Sttt) / denom

End Function
```

Appendix B: Listing of FADD2D input deck for stress analysis of a quasi-rectangular hole with ε = –0.0876 and α = 0.5269

The following is a listing of the FADD2D input deck that was used to determine the stress distribution around a quasi-rectangular hole in an infinite plate in order to compare to the results produced by the equations published by Rajaiah and Naik (1983). In this particular instance, the shape parameters of the quasi-rectangular hole were ε = –0.0876 and α = 0.5269, and a remote reversed biaxial loading of σ_x = 100 MPa and σ_y = –100 MPa was specified (corresponding to σ_x:σ_y = 1:–1). The geometry of the hole in the model was scaled in such a way that the maximum x-dimension of the hole was 91.240 mm and the maximum y-dimension was 45.631 mm. The aspect ratio of the hole was therefore l:w = 1.9995:1 ≈ 2:1. Note that at x = 0, the y-coordinates of the hole are ±43.930 mm, so the hole is narrower towards the middle section (see Figure 4a).

```
FADD - Visual C++ Version 1.0 - 01/30/15
Elongated Quasi-Rectangular Hole
Infinite Domain Example
-----------------------------------------------------
Problem Type, No of Materials
4 1
Material, SigXX, SigYY, SigXY, Zx, Zy,
1 100.000000 -100.000000 0.000000 0.000000 0.000000
Materials, Elastic modulus, and Poisson's ratio
1 70000.000000 0.330000
Material, Cracks, Boundaries, and Point loads
1 0 1 0
 Input echo, Boundary Stresses, and Displacements
1 1 1

-----------------------------------------------------
Definition of Boundary

1 1
0 0 36

01 1 2
   0.91240000E+2  0.00000000E+2 -1 0.000000 -1 0.000000 0
   0.91157960E+2  0.06859491E+2 -1 0.000000 -1 0.000000 0
   0.90894393E+2  0.13529522E+2 -1 0.000000 -1 0.000000 0

02 1 2
   0.90894393E+2  0.13529522E+2 -1 0.000000 -1 0.000000 0
   0.90398327E+2  0.19831431E+2 -1 0.000000 -1 0.000000 0
   0.89589262E+2  0.25607424E+2 -1 0.000000 -1 0.000000 0

03 1 2
   0.89589262E+2  0.25607424E+2 -1 0.000000 -1 0.000000 0
   0.88363524E+2  0.30729266E+2 -1 0.000000 -1 0.000000 0
   0.86602540E+2  0.35105000E+2 -1 0.000000 -1 0.000000 0

04 1 2
   0.86602540E+2  0.35105000E+2 -1 0.000000 -1 0.000000 0
   0.84182459E+2  0.38683253E+2 -1 0.000000 -1 0.000000 0
   0.80984444E+2  0.41454862E+2 -1 0.000000 -1 0.000000 0

05 1 2
   0.80984444E+2  0.41454862E+2 -1 0.000000 -1 0.000000 0
   0.76904934E+2  0.43451712E+2 -1 0.000000 -1 0.000000 0
   0.71865144E+2  0.44742882E+2 -1 0.000000 -1 0.000000 0
```

```
06 1 2
   0.71865144E+2  0.44742882E+2 -1 0.000000 -1 0.000000 0
   0.65819154E+2  0.45428376E+2 -1 0.000000 -1 0.000000 0
   0.58760000E+2  0.45630879E+2 -1 0.000000 -1 0.000000 0

07 1 2
   0.58760000E+2  0.45630879E+2 -1 0.000000 -1 0.000000 0
   0.50723336E+2  0.45486102E+2 -1 0.000000 -1 0.000000 0
   0.41788397E+2  0.45132404E+2 -1 0.000000 -1 0.000000 0

08 1 2
   0.41788397E+2  0.45132404E+2 -1 0.000000 -1 0.000000 0
   0.32076160E+2  0.44700376E+2 -1 0.000000 -1 0.000000 0
   0.21744818E+2  0.44303138E+2 -1 0.000000 -1 0.000000 0

09 1 2
   0.21744818E+2  0.44303138E+2 -1 0.000000 -1 0.000000 0
   0.10982829E+2  0.44027988E+2 -1 0.000000 -1 0.000000 0
   0.00000000E+2  0.43930000E+2 -1 0.000000 -1 0.000000 0

10 1 2
   0.00000000E+2  0.43930000E+2 -1 0.000000 -1 0.000000 0
  -0.10982829E+2  0.44027988E+2 -1 0.000000 -1 0.000000 0
  -0.21744818E+2  0.44303138E+2 -1 0.000000 -1 0.000000 0

11 1 2
  -0.21744818E+2  0.44303138E+2 -1 0.000000 -1 0.000000 0
  -0.32076160E+2  0.44700376E+2 -1 0.000000 -1 0.000000 0
  -0.41788397E+2  0.45132404E+2 -1 0.000000 -1 0.000000 0

12 1 2
  -0.41788397E+2  0.45132404E+2 -1 0.000000 -1 0.000000 0
  -0.50723336E+2  0.45486102E+2 -1 0.000000 -1 0.000000 0
  -0.58760000E+2  0.45630879E+2 -1 0.000000 -1 0.000000 0

13 1 2
  -0.58760000E+2  0.45630879E+2 -1 0.000000 -1 0.000000 0
  -0.65819154E+2  0.45428376E+2 -1 0.000000 -1 0.000000 0
  -0.71865144E+2  0.44742882E+2 -1 0.000000 -1 0.000000 0

14 1 2
  -0.71865144E+2  0.44742882E+2 -1 0.000000 -1 0.000000 0
  -0.76904934E+2  0.43451712E+2 -1 0.000000 -1 0.000000 0
  -0.80984444E+2  0.41454862E+2 -1 0.000000 -1 0.000000 0

15 1 2
  -0.80984444E+2  0.41454862E+2 -1 0.000000 -1 0.000000 0
  -0.84182459E+2  0.38683253E+2 -1 0.000000 -1 0.000000 0
  -0.86602540E+2  0.35105000E+2 -1 0.000000 -1 0.000000 0

16 1 2
  -0.86602540E+2  0.35105000E+2 -1 0.000000 -1 0.000000 0
  -0.88363524E+2  0.30729266E+2 -1 0.000000 -1 0.000000 0
  -0.89589262E+2  0.25607424E+2 -1 0.000000 -1 0.000000 0

17 1 2
  -0.89589262E+2  0.25607424E+2 -1 0.000000 -1 0.000000 0
  -0.90398327E+2  0.19831431E+2 -1 0.000000 -1 0.000000 0
  -0.90894393E+2  0.13529522E+2 -1 0.000000 -1 0.000000 0

18 1 2
  -0.90894393E+2  0.13529522E+2 -1 0.000000 -1 0.000000 0
  -0.91157960E+2  0.06859491E+2 -1 0.000000 -1 0.000000 0
  -0.91240000E+2  0.00000000E+2 -1 0.000000 -1 0.000000 0

19 1 2
  -0.91240000E+2  0.00000000E+2 -1 0.000000 -1 0.000000 0
  -0.91157960E+2 -0.06859491E+2 -1 0.000000 -1 0.000000 0
```

```
  -0.90894393E+2 -0.13529522E+2 -1 0.000000 -1 0.000000 0

20 1 2
  -0.90894393E+2 -0.13529522E+2 -1 0.000000 -1 0.000000 0
  -0.90398327E+2 -0.19831431E+2 -1 0.000000 -1 0.000000 0
  -0.89589262E+2 -0.25607424E+2 -1 0.000000 -1 0.000000 0

21 1 2
  -0.89589262E+2 -0.25607424E+2 -1 0.000000 -1 0.000000 0
  -0.88363524E+2 -0.30729266E+2 -1 0.000000 -1 0.000000 0
  -0.86602540E+2 -0.35105000E+2 -1 0.000000 -1 0.000000 0

22 1 2
  -0.86602540E+2 -0.35105000E+2 -1 0.000000 -1 0.000000 0
  -0.84182459E+2 -0.38683253E+2 -1 0.000000 -1 0.000000 0
  -0.80984444E+2 -0.41454862E+2 -1 0.000000 -1 0.000000 0

23 1 2
  -0.80984444E+2 -0.41454862E+2 -1 0.000000 -1 0.000000 0
  -0.76904934E+2 -0.43451712E+2 -1 0.000000 -1 0.000000 0
  -0.71865144E+2 -0.44742882E+2 -1 0.000000 -1 0.000000 0

24 1 2
  -0.71865144E+2 -0.44742882E+2 -1 0.000000 -1 0.000000 0
  -0.65819154E+2 -0.45428376E+2 -1 0.000000 -1 0.000000 0
  -0.58760000E+2 -0.45630879E+2 -1 0.000000 -1 0.000000 0

25 1 2
  -0.58760000E+2 -0.45630879E+2 -1 0.000000 -1 0.000000 0
  -0.50723336E+2 -0.45486102E+2 -1 0.000000 -1 0.000000 0
  -0.41788397E+2 -0.45132404E+2 -1 0.000000 -1 0.000000 0

26 1 2
  -0.41788397E+2 -0.45132404E+2 -1 0.000000 -1 0.000000 0
  -0.32076160E+2 -0.44700376E+2 -1 0.000000 -1 0.000000 0
  -0.21744818E+2 -0.44303138E+2 -1 0.000000 -1 0.000000 0

27 1 2
  -0.21744818E+2 -0.44303138E+2 -1 0.000000 -1 0.000000 0
  -0.10982829E+2 -0.44027988E+2 -1 0.000000 -1 0.000000 0
   0.00000000E+2 -0.43930000E+2 -1 0.000000 -1 0.000000 0

28 1 2
   0.00000000E+2 -0.43930000E+2 -1 0.000000 -1 0.000000 0
   0.10982829E+2 -0.44027988E+2 -1 0.000000 -1 0.000000 0
   0.21744818E+2 -0.44303138E+2 -1 0.000000 -1 0.000000 0

29 1 2
   0.21744818E+2 -0.44303138E+2 -1 0.000000 -1 0.000000 0
   0.32076160E+2 -0.44700376E+2 -1 0.000000 -1 0.000000 0
   0.41788397E+2 -0.45132404E+2 -1 0.000000 -1 0.000000 0

30 1 2
   0.41788397E+2 -0.45132404E+2 -1 0.000000 -1 0.000000 0
   0.50723336E+2 -0.45486102E+2 -1 0.000000 -1 0.000000 0
   0.58760000E+2 -0.45630879E+2 -1 0.000000 -1 0.000000 0

31 1 2
   0.58760000E+2 -0.45630879E+2 -1 0.000000 -1 0.000000 0
   0.65819154E+2 -0.45428376E+2 -1 0.000000 -1 0.000000 0
   0.71865144E+2 -0.44742882E+2 -1 0.000000 -1 0.000000 0

32 1 2
   0.71865144E+2 -0.44742882E+2 -1 0.000000 -1 0.000000 0
   0.76904934E+2 -0.43451712E+2 -1 0.000000 -1 0.000000 0
   0.80984444E+2 -0.41454862E+2 -1 0.000000 -1 0.000000 0

33 1 2
   0.80984444E+2 -0.41454862E+2 -1 0.000000 -1 0.000000 0
```

```
   0.84182459E+2 -0.38683253E+2 -1 0.000000 -1 0.000000 0
   0.86602540E+2 -0.35105000E+2 -1 0.000000 -1 0.000000 0

34 1 2
   0.86602540E+2 -0.35105000E+2 -1 0.000000 -1 0.000000 0
   0.88363524E+2 -0.30729266E+2 -1 0.000000 -1 0.000000 0
   0.89589262E+2 -0.25607424E+2 -1 0.000000 -1 0.000000 0

35 1 2
   0.89589262E+2 -0.25607424E+2 -1 0.000000 -1 0.000000 0
   0.90398327E+2 -0.19831431E+2 -1 0.000000 -1 0.000000 0
   0.90894393E+2 -0.13529522E+2 -1 0.000000 -1 0.000000 0

36 1 2
   0.90894393E+2 -0.13529522E+2 -1 0.000000 -1 0.000000 0
   0.91157960E+2 -0.06859491E+2 -1 0.000000 -1 0.000000 0
   0.91240000E+2  0.00000000E+2 -1 0.000000 -1 0.000000 0

-----------------------------------------------------------
```

Appendix C: Fortran program for computing stress-minimised quasi-rectangular hole shapes under biaxial loading

C.1. Description

The following program is written in FORTRAN 90. It can be used to calculate sets of tables of stress-minimised quasi-rectangular holes which are a function of the aspect ratio of the hole. The equations used for computing the stress distribution around a quasi-rectangular hole are based on the publication by Rajaiah and Naik (1983). An additional equation has been implemented to enable the direct analytical computation of the radius of curvature around the hole boundary.

The output file `quasirecttables.out` stores the results tables corresponding to each specific biaxial loading case that is specified in the program. Each line in these tables contains the values of the shape parameters ε (`eps`) and α (`alpha`) for each stress-minimised quasi-rectangular hole determined for the selected values of hole aspect ratio, as well as the maximum and minimum K_t values, the maximum x- and y-values for the shape, the minimum and maximum radius-of-curvature values, and the ratio of the minimum radius-of-curvature to the width w of the hole. Each line also includes data for an elliptical hole with the same aspect ratio. Note that the format of the tables produced by `quasirecttables.out` is similar to that which is used in Tables 3–8 in this document. The layout of the tables is also designed to make them amenable to pasting into a spreadsheet for the purpose of plotting out the results.

C.2. Source code listing

```
!=============================================================================================

program StressMinimiseQuasiRectangle

real timebeg,timeend

call cpu_time(timebeg)

call ComputeQuasiRectTables

write(*,*)

call cpu_time(timeend)

write(*,'(a,f10.2,a)') 'CPU Time = ',(timeend-timebeg)/60.0d0, ' minutes'

write(*,*)

stop
end

!=============================================================================================

subroutine StQuasiRect(r,eps,alpha,sx,sy,theta,d,thetaxy,x,y,st,stx,sty,radcurv)

! Tangential stress around boundary of a quasi-rectangular hole when the
! plate is subjected to uniform tension stresses of Sx and Sy.
!
```

```
! Rajaiah K, Naik NK. Hole shapes with minimum stress concentration in
! infinite isotropic plates using conformal transformation. ISME Journal
! of Engineering Design, Vol 1, No 1, April 1983, pp 15-19.

implicit none

real(8) r,eps,alpha,theta,sx,sy,d,thetaxy,x,y,st,stx,sty,radcurv

real(8) a,b,c2,cost,sint,cos3t,sin3t,alphap1

real(8) ROC

cost  = cosd(theta)
sint  = sind(theta)
cos3t = cosd(3.0d0*theta)
sin3t = sind(3.0d0*theta)

x = r*(      cost+eps*cos3t)
y = r*(alpha*sint-eps*sin3t)

a = alpha*cost-3.0d0*eps*cos3t
b =       sint+3.0d0*eps*sin3t

c2 = a**2+b**2

alphap1 = 1.0d0+alpha

! Tangential stress around hole for tension aligned with x-axis.

stx = (b**2/c2)+(1.0d0/c2)*(alpha*(-a*cost                              &
      +2.0d0*b*sint)-eps*(4.0d0*a*alpha*cost/alphap1                    &
      -3.0d0*a*cos3t+2.0d0*b*(-2.0d0*alpha*sint/alphap1+3.0d0*sin3t)) &
      -8.0d0*eps**2*alpha/alphap1**2*(a*cost-b*sint))

! Tangential stress around hole for tension aligned with y-axis.

sty = (a**2/c2)+(1.0d0/c2)*(2.0d0*a*cost                    &
      -b*sint+eps*(2.0d0*a*(2.0d0*cost/alphap1              &
      +3.0d0*cos3t)-4.0d0*b*sint/alphap1-3.0d0*b*sin3t)     &
      +8.0d0*eps**2/alphap1**2*(a*cost-b*sint))

st = stx*sx + sty*sy

! Compute the actual geometric theta from the (x,y) coordinates.

thetaxy = atan2d(y,x)

d = sqrt(x**2+y**2)

! Compute the local radius of curvature of the shape.

radcurv = ROC(r,eps,alpha,theta)

return
end

!===============================================================================

real(8) function ROC(r,eps,alpha,tdeg)

! Compute the radius of curvature of the quasi-rectangular shape.

implicit none

real(8) r,eps,alpha,tdeg
real(8) xd1,xd2,yd1,yd2,sint,cost,sin3t,cos3t

sint  = sind(tdeg)
cost  = cosd(tdeg)
```

```
sin3t = sind(3.0d0*tdeg)
cos3t = cosd(3.0d0*tdeg)

xd1 = r*(-sint - 3.0d0*eps*sin3t)
xd2 = r*(-cost - 9.0d0*eps*cos3t)
yd1 = r*( alpha*cost - 3.0d0*eps*cos3t)
yd2 = r*(-alpha*sint + 9.0d0*eps*sin3t)

ROC = abs((xd1**2 + yd1**2)**1.5d0/(xd1*yd2 - yd1*xd2))

return
end


!=======================================================================================

subroutine ComputeSt(r,eps,alpha,sx,sy,thetabeg,thetaend,n,stmin,thetamin, &
                     stmax,thetamax,xmax,ymax,s,rcmin,rcmax,rcminonw)

! Compute the minimum and maximum tangential stresses occurring around the
! boundary of the quasi-rectangular hole. Also compute the locations of
! those stresses, as well as the minimum and maximum radius of curvature
! values.

integer n
real(8) r,eps,alpha,sx,sy,thetabeg,thetaend
real(8) stmin,thetamin,stmax,thetamax,xmax,ymax,s,rcmin,rcmax,rcminonw

real(8) st,stx,sty,theta,dtheta,thetaxy,x,y,d,xold,yold,rc
integer i

dtheta=(thetaend-thetabeg)/(n-1)

do i=1,n

  if (i==1) then
    theta=thetabeg
  else if (i==n) then
    theta=thetaend
  else
    theta=thetabeg+(i-1)*dtheta
  endif

  call StQuasiRect(r,eps,alpha,sx,sy,theta,d,thetaxy,x,y,st,stx,sty,rc)

  if (i==1) then
    stmin    = st
    stmax    = st
    xmax     = abs(x)
    ymax     = abs(y)
    thetamin = theta
    thetamax = theta
    rcmin    = rc
    rcmax    = rc
  endif

  if (st>stmax) then
    stmax=st
    thetamax=theta
  endif

  if (st<stmin) then
    stmin=st
    thetamin=theta
  endif

  xmax=max(abs(x),xmax)
  ymax=max(abs(y),ymax)
```

```
      rcmin = min(rc,rcmin)
      rcmax = max(rc,rcmax)

      if (i==1) then
        s=0.0d0
        xold=x
        yold=y
      else
        s=s+sqrt((x-xold)**2+(y-yold)**2)
        xold=x
        yold=y
      endif

    enddo

    rcminonw = rcmin/(2.0d0*ymax)

    return
    end

    !=============================================================================================

    subroutine ComputeQuasiRectTables

    implicit none

    integer, parameter:: luo1=10
    integer, parameter:: luo2=11
    integer, parameter:: maxcases=20

    real(8)   r,eps,alpha,thetabeg,thetaend
    real(8)   s,els,xmax,ymax,elxmax,elymax
    real(8)   thetamin,thetamax,stmin,stmax,xmaxonymax,ratio
    real(8)   elthetamin,elthetamax,elstmin,elstmax,elrcminonw
    real(8)   xmaxonymax0,eps0,alpha0,stmax0,stmin0,xmax0,ymax0
    real(8)   eleps0,elalpha0,elstmax0,elstmin0,elxmax0,elymax0
    real(8)   rcmin,rcmax,rcminonw,rcmin0,rcmax0,rcminonw0
    real(8)   elrcmin0,elrcmax0,elrcminonw0
    real(8)   alpha1,alpha2
    real(8)   sx(maxcases),sy(maxcases)
    integer   i,ncases,iratio,ieps,ialpha
    integer   ipeak(maxcases),np(maxcases)

    open(unit=luo1,file='quasirectlocate.out',status='unknown')
    open(unit=luo2,file='quasirecttables.out',status='unknown')

    ! Define the biaxial loading cases below, taking care not to have
    ! more than maxcases.

    i=0;

    i=i+1; ipeak(i) = 2; sx(i) = +1.0000d0; sy(i) =  0.0000d0; np(i)=721
    i=i+1; ipeak(i) = 2; sx(i) =  0.0000d0; sy(i) = +1.0000d0; np(i)=721
    i=i+1; ipeak(i) = 1; sx(i) = +1.0000d0; sy(i) = -1.0000d0; np(i)=721
    i=i+1; ipeak(i) = 1; sx(i) = -1.0000d0; sy(i) = +1.0000d0; np(i)=721
    i=i+1; ipeak(i) = 2; sx(i) = +1.3770d0; sy(i) = -1.0000d0; np(i)=721
    i=i+1; ipeak(i) = 2; sx(i) = +1.0000d0; sy(i) = +1.0000d0; np(i)=721
    i=i+1; ipeak(i) = 2; sx(i) = +2.0000d0; sy(i) = +1.0000d0; np(i)=721
    i=i+1; ipeak(i) = 2; sx(i) = +3.0000d0; sy(i) = +1.0000d0; np(i)=721
    i=i+1; ipeak(i) = 2; sx(i) = +4.0000d0; sy(i) = +1.0000d0; np(i)=721

    ncases = i

    r        =  1.0d0
    thetabeg =  0.0d0
    thetaend = 90.0d0

    do i = 1,ncases
      write(*,'(2(a,f8.4))') 'Computing results for: Sx = ',sx(i),' Sy = ',sy(i)
```

```
write(*,*)
write(*,'(10a15)') 'Xmax/Ymax','eps','alpha','Stmax','Stmin','Xmax','Ymax', &
                   'ROCmin','ROCmax','ROCmin/w'
write(luo2,'(a)') &
  '--------------------------------------------------------------------------'
write(luo2,*)
write(luo2,'(a,f8.4)') 'Sx = ',sx(i)
write(luo2,'(a,f8.4)') 'Sy = ',sy(i)
write(luo2,*)
write(luo2,'(20a15)') 'Xmax/Ymax','eps','alpha','Stmax','Stmin','Xmax','Ymax',      &
                      'ROCmin','ROCmax','ROCmin/w','ElXmax/Ymax','Eleps','Elalpha', &
                      'ElStmax','ElStmin','ElXmax','ElYmax','ElROCmin','ElROCmax',  &
                      'ElROCmin/w'
do iratio = 100,500,25
  ratio = iratio/100.0d0
  write(luo1,'(a)') &
    '--------------------------------------------------------------------------'
  write(luo1,*)
  write(luo1,'(a,f8.4)') 'Aspect Ratio = ',ratio
  write(luo1,'(a,f8.4)') 'Sx           = ',sx(i)
  write(luo1,'(a,f8.4)') 'Sy           = ',sy(i)
  write(luo1,*)
  write(luo1,'(10a15)') 'Xmax/Ymax','eps','alpha','Stmax','Stmin','Xmax','Ymax', &
                        'ROCmin','ROCmax','ROCmin/w'
  stmax0 = +1.0d99
  stmin0 = -1.0d99
  do ieps=0,-1200,-1
    eps=ieps/10000.0d0
    alpha1 = 0.90d0/ratio
    alpha2 = 1.10d0/ratio
    if (alpha2>1.0d0) then
      alpha2 = 1.0d0
      alpha1 = 0.80d0/ratio
    endif
    do ialpha=nint(alpha1*10000.0d0),nint(alpha2*10000.0d0),1
      alpha=ialpha/10000.0d0
      call ComputeSt(r,eps,alpha,sx(i),sy(i),thetabeg,thetaend,np(i),stmin,thetamin, &
                     stmax,thetamax,xmax,ymax,s,rcmin,rcmax,rcminonw)
      xmaxonymax=xmax/ymax
      if (abs(xmaxonymax-ratio)<0.0005d0) then
        write(luo1,'(9f15.5)') xmaxonymax,eps,alpha,stmax,stmin,xmax,ymax,rcmin,rcmax
        if (ipeak(i)==2) then
          if (max(abs(stmax),abs(stmin))<max(abs(stmax0),abs(stmin0))) then
            stmax0      = stmax
            stmin0      = stmin
            xmaxonymax0 = xmaxonymax
            eps0        = eps
            alpha0      = alpha
            rcmin0      = rcmin
            rcmax0      = rcmax
            xmax0       = xmax
            ymax0       = ymax
            rcminonw0   = rcminonw
          endif
        else if (ipeak(i)==1) then
          if (abs(stmin)<abs(stmin0)) then
            stmax0      = stmax
            stmin0      = stmin
            xmaxonymax0 = xmaxonymax
            eps0        = eps
            alpha0      = alpha
            rcmin0      = rcmin
            rcmax0      = rcmax
            xmax0       = xmax
            ymax0       = ymax
            rcminonw0   = rcminonw
          endif
        else
          stop 'Invalid value of ipeak.'
```

```
            endif
          endif
        enddo
      enddo
      write(luo1,*)
      write(luo1,*) 'Values at minimum St:'
      write(luo1,*)
      write(luo1,'(10f15.5)') xmaxonymax0,eps0,alpha0,stmax0,stmin0,xmax0,ymax0, &
                              rcmin0,rcmax0,rcminonw0
      write(*,'(10f15.5,a)') xmaxonymax0,eps0,alpha0,stmax0,stmin0, &
                             xmax0,ymax0,rcmin0,rcmax0,rcminonw0,' -- optimal shape'
      eleps0   = 0.0d0
      elalpha0 = 1.0d0/ratio
      call ComputeSt(r,eleps0,elalpha0,sx(i),sy(i),thetabeg,thetaend,np(i), &
                     elstmin0,elthetamin,elstmax0,elthetamax,elxmax,elymax, &
                     els,elrcmin0,elrcmax0,elrcminonw0)
      write(*,'(10f15.5,a)') elxmax/elymax,eleps0,elalpha0,elstmax0,elstmin0, &
                             elxmax,elymax,elrcmin0,elrcmax0,elrcminonw0,     &
                             ' -- elliptical shape'
      write(luo1,*)
      write(luo1,*) 'Values for elliptical shape:'
      write(luo1,*)
      write(luo1,'(10f15.5)') elxmax/elymax,eleps0,elalpha0,elstmax0,elstmin0, &
                              elxmax,elymax,elrcmin0,elrcmax0,elrcminonw
      write(luo1,*)
      write(luo2,'(20f15.5)') xmaxonymax0,eps0,alpha0,stmax0,stmin0,xmax0,ymax0,rcmin0, &
                              rcmax0,rcminonw0,elxmax/elymax,eleps0,elalpha0,elstmax0,  &
                              elstmin0,elxmax,elymax,elrcmin0,elrcmax0,elrcminonw0
    enddo
    write(*,*)
    write(luo2,*)
  enddo

  close(luo1)
  close(luo2)

  return
  end
```

DISTRIBUTION LIST

Determination of Minimised K_t Values and Boundary Shapes
for a Class of Quasi-Rectangular Holes in Infinite Plates

Witold Waldman

AUSTRALIA

DEFENCE ORGANISATION	**No. of Copies**
Task Sponsor	
OIC-ASI-DGTA	1
S&T Program	
Air Force Scientific Adviser	1
Navy Scientific Adviser	1
Chief of Aerospace Division	1
Research Leader, Airframe Technology and Safety Branch	1
Research Leader, Aircraft Structures Branch	1
Research Leader, Aircraft Health and Sustainment Branch	1
Witold Waldman (Author)	1
Science Team Leader, Structural Mechanics	1
Manfred Heller	1
Rebecca Evans	1
Kevin Walker	1
Michael Opie	1
Andrew Gregory	1
Stephen Sanderson	1
Weiping Hu	1
Chris Wallbrink	1
Madeleine Burchill	1
John Wang	1
Ben Dixon	1
DST Group Library	
Library, Edinburgh	1
UNIVERSITIES AND COLLEGES	
Monash University	
Professor Rhys Jones, Department of Mechanical and Aerospace Engineering	1
Professor Wing Kong Chiu, Department of Mechanical and Aerospace Engineering	1
RMIT University	
Professor Chun Wang, School of Aerospace, Mechanical and Manufacturing Engineering	1
Professor Adrian Mouritz, School of Aerospace, Mechanical and Manufacturing Engineering	1

OUTSIDE AUSTRALIA

UNIVERSITIES AND COLLEGES

Mississippi State University
Professor James C. Newman, Jr, Department of Aerospace Engineering 1

The University of Texas at Austin
Professor Mark E. Mear, Department of Aerospace Engineering and Engineering Mechanics 1

OTHER ORGANISATIONS

ESDU, IHS Global Limited 1
Dr Dorothy Downs

Total number of copies: 28

DEFENCE SCIENCE AND TECHNOLOGY GROUP
DOCUMENT CONTROL DATA

1. DLM/CAVEAT (OF DOCUMENT)

2. TITLE

Determination of Minimised K_t Values and Boundary Shapes for a Class of Quasi-Rectangular Holes in Infinite Plates

3. SECURITY CLASSIFICATION (FOR UNCLASSIFIED REPORTS THAT ARE LIMITED RELEASE USE (L) NEXT TO DOCUMENT CLASSIFICATION)

Document (U)
Title (U)
Abstract (U)

4. AUTHOR(S)

Witold Waldman

5. CORPORATE AUTHOR

Defence Science and Technology Group
506 Lorimer St
Fishermans Bend Victoria 3207 Australia

6a. DST GROUP NUMBER	6b. AR NUMBER	6c. TYPE OF REPORT	7. DOCUMENT DATE
DST Group-TR-3125	AR-016-304	Technical Report	July 2015

8. FILE NUMBER	9. TASK NUMBER	10. TASK SPONSOR	11. NO. OF PAGES	12. NO. OF REFERENCES
2015/1025296/1	AIR 07/283	OIC-ASI-DGTA	50	25

13. DST GROUP PUBLICATIONS REPOSITORY

http://dspace.dsto.defence.gov.au/dspace/

14. RELEASE AUTHORITY

Chief, Aerospace Division

15. SECONDARY RELEASE STATEMENT OF THIS DOCUMENT

Approved for public release

OVERSEAS ENQUIRIES OUTSIDE STATED LIMITATIONS SHOULD BE REFERRED THROUGH DOCUMENT EXCHANGE, PO BOX 1500, EDINBURGH, SA 5111

16. DELIBERATE ANNOUNCEMENT

No Limitations

17. CITATION IN OTHER DOCUMENTS

Yes

18. DST GROUP RESEARCH LIBRARY THESAURUS

Shape optimisation, Quasi-rectangular shapes, Holes, Stress concentration, Fatigue life extension, Boundary element method, Numerical modelling, Numerical simulation, Aircraft structure

19. ABSTRACT

Transferable solutions for stress-minimised quasi-rectangular holes in a two-dimensional infinite plate have been determined for a number of remote loading conditions and a wide range of hole aspect ratios. These include uniaxial, equibiaxial and reversed biaxial loading cases. The analytical shape and tangential stress equations for these quasi-rectangular holes can readily be used to obtain solutions for other specific biaxial loading cases that are of interest. The equation for the radius of curvature for these shapes has also been derived. Tables and plots of shape parameters and stress concentration factors are provided, enabling the stress-minimised quasi-rectangular hole shapes to be easily and rapidly applied by designers. These shapes produce peak stresses that are often within 10% of those obtained by free-form shape optimisation, and they can serve as initial shapes for subsequent free-form shape optimisation analyses. The source code for the program that was used to determine the stress-minimised quasi-rectangular hole shapes as a function of hole aspect ratio is provided, as is a set of functions that are suitable for use in spreadsheets. For the first time, these tools provide an automated procedure that enables a designer to set up a biaxial loading condition of interest and then determine sets of stress-minimised quasi-rectangular hole shapes that vary as a function of hole aspect ratio.